

The Offshore Palos Verdes Fault Zone near San Pedro, Southern California

by Michael A. Fisher, William R. Normark, Victoria E. Langenheim, Andrew J. Calvert,
and Ray Sliter

Abstract High-resolution seismic-reflection data are combined with a variety of other geophysical and geological data to interpret the offshore structure and earthquake hazards of the San Pedro shelf, near Los Angeles, California. Prominent structures investigated include the Wilmington graben, the Palos Verdes fault zone, various faults below the west part of the San Pedro shelf and slope, and the deep-water San Pedro basin. The structure of the Palos Verdes fault zone changes markedly along strike southeastward across the San Pedro shelf and slope. Under the north part of the shelf, this fault zone includes several strands, with the main strand dipping west. Under the slope, the main fault strands exhibit normal separation and mostly dip east. To the southeast near Lasuen Knoll, the Palos Verdes fault zone locally is low angle, but elsewhere near this knoll, the fault dips steeply. Fresh seafloor scarps near Lasuen Knoll indicate recent fault movement. We explain the observed structural variation along the Palos Verdes fault zone as the result of changes in strike and fault geometry along a master right-lateral strike-slip fault at depth. Complicated movement along this deep fault zone is suggested by the possible wave-cut terraces on Lasuen Knoll, which indicate subaerial exposure during the last sea level lowstand and subsequent subsidence of the knoll. Modeling of aeromagnetic data indicates a large magnetic body under the west part of the San Pedro shelf and upper slope. We interpret this body to be thick basalt of probable Miocene age. This basalt mass appears to have affected the pattern of rock deformation, perhaps because the basalt was more competent during deformation than the sedimentary rocks that encased the basalt. West of the Palos Verdes fault zone, other northwest-striking faults deform the outer shelf and slope. Evidence for recent movement along these faults is equivocal, because we lack age dates on deformed or offset sediment.

Introduction

Numerous thrust and strike-slip faults crosscut the region that includes the city of Los Angeles, southern California (Fig. 1), and they pose a significant earthquake hazard to this burgeoning population center (e.g., Wright, 1991; Dolan *et al.*, 2000). Much effort has been expended to locate and determine the displacement history of these faults; even so, a category of fault that remains poorly understood includes active offshore faults within about 50 km of the coast. Largely because of a lack of information, such faults are often omitted from models of tectonic evolution and estimates of regional seismic hazard.

Historical seismicity indicates that offshore faults can unleash earthquakes with at least moderate magnitude (Astiz and Shearer, 2000). In 1933, a large (M_w 6.4) offshore earthquake near Long Beach probably struck along the Newport–Inglewood fault (Barrows, 1974; Hauksson and Gross, 1991). Offshore epicenters in and around the study area are diffuse but tend to cluster over the western San Pedro shelf and eastern San Pedro Basin (Fig. 1). Two moderate, off-

shore earthquakes (M 5.2 in 1979 and M 5.0 in 1989) occurred near the coastal town of Malibu (Hauksson and Saldivar, 1986; Johnson and Acosta, 1989) (see inset to Fig. 1). No large earthquakes have occurred along the Palos Verdes fault zone, which strikes generally southeast across the study area (Fig. 1). However, McNeilan *et al.* (1996) estimated that this fault could produce an earthquake as large as M 7.

The dearth of information about Holocene activity along offshore faults provided the impetus to study the geologic structure offshore from southern California. During 1998 through 2000, the U.S. Geological Survey (USGS) collected high- and medium-resolution, marine seismic-reflection data (Fig. 2) with the goal of locating active faults and estimating their displacement histories. A related research goal is understanding the susceptibility of the offshore region to earthquake-induced landslides and consequent local tsunamis. The Portuguese Bend landslide on the Palos Verdes Peninsula (e.g., Woodring *et al.*, 1946) and offshore landslides evident in seismic-reflection and multibeam bathymetric

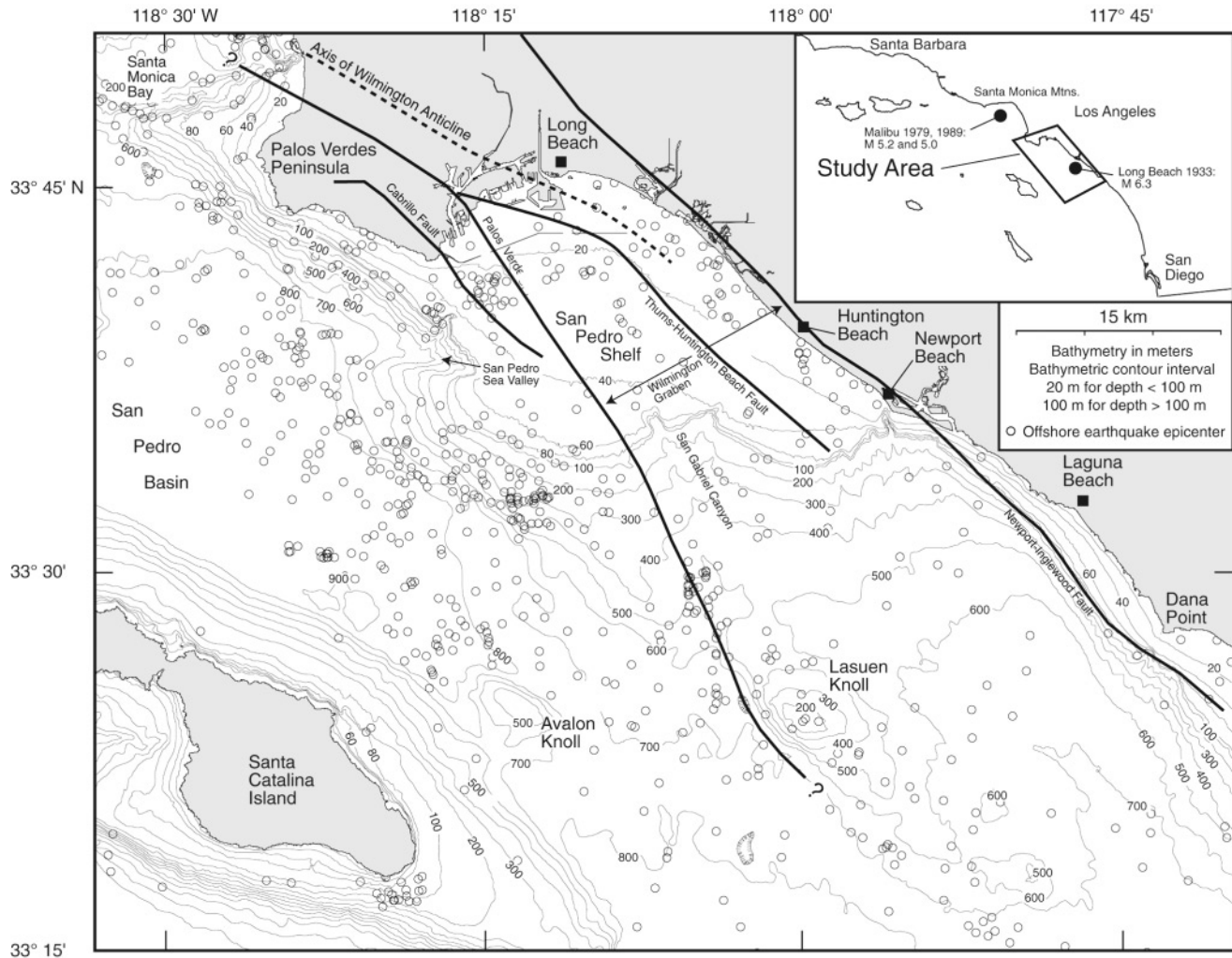


Figure 1. Location of the study area near the San Pedro shelf, as well as the main faults, epicenters (epoch 1978–1998; Astiz and Shearer [2000]), and bathymetry. The short-dashed line labeled “WA” shows the axis of the Wilmington anticline.

data (e.g., Locat and Lee, 2002) indicate that local sediment bodies under the seafloor are susceptible to catastrophic downslope movement.

In this article, we focus on the offshore structure and stratigraphy southeastward from the Palos Verdes Peninsula to near Dana Point (Fig. 1). This area includes the Palos Verdes (Fischer *et al.*, 1987; McNeilan *et al.*, 1996) and Newport–Inglewood faults (Barrows, 1974; Fischer, 1992) that are thought to play key roles in the regional earthquake hazard. In particular, we document the detailed changes in structure along the strike of the offshore Palos Verdes fault zone.

Geophysical Data

Seismic-Reflection Data

Multichannel seismic (MCS) reflection data used herein (Fig. 2) were collected by the USGS during three cruises (Normark *et al.*, 1999a,b; Gutmacher *et al.*, 2000). The seis-

mic system included a 24-channel streamer with 10-m-long hydrophone sections. The resulting, 5-m common-depth-point interval provided high spatial resolution. The sound source was a dual-chambered generator-injector airgun; both chambers had a volume of 35 in³. The airgun was suspended from a float to maintain a constant source depth of 1 m, and the airgun was fired every 12 sec with an air pressure of 3000 psi.

Deep-crustal MCS data, collected in 1994 off southern California for the Los Angeles Regional Seismic Experiment (LARSE) (see Fig. 2 for seismic line location) (Brocher *et al.*, 1995), are 40-fold and were collected aboard the R/V *Maurice Ewing*, using a source array of 20 airguns with a total chamber volume of 137.7 L (8470 in³). The digital streamer was 4200 m long and had 160 data channels.

Potential-Field Data

Offshore aeromagnetic data were obtained during a regional survey (Langenheim *et al.*, 1993) flown along flight-

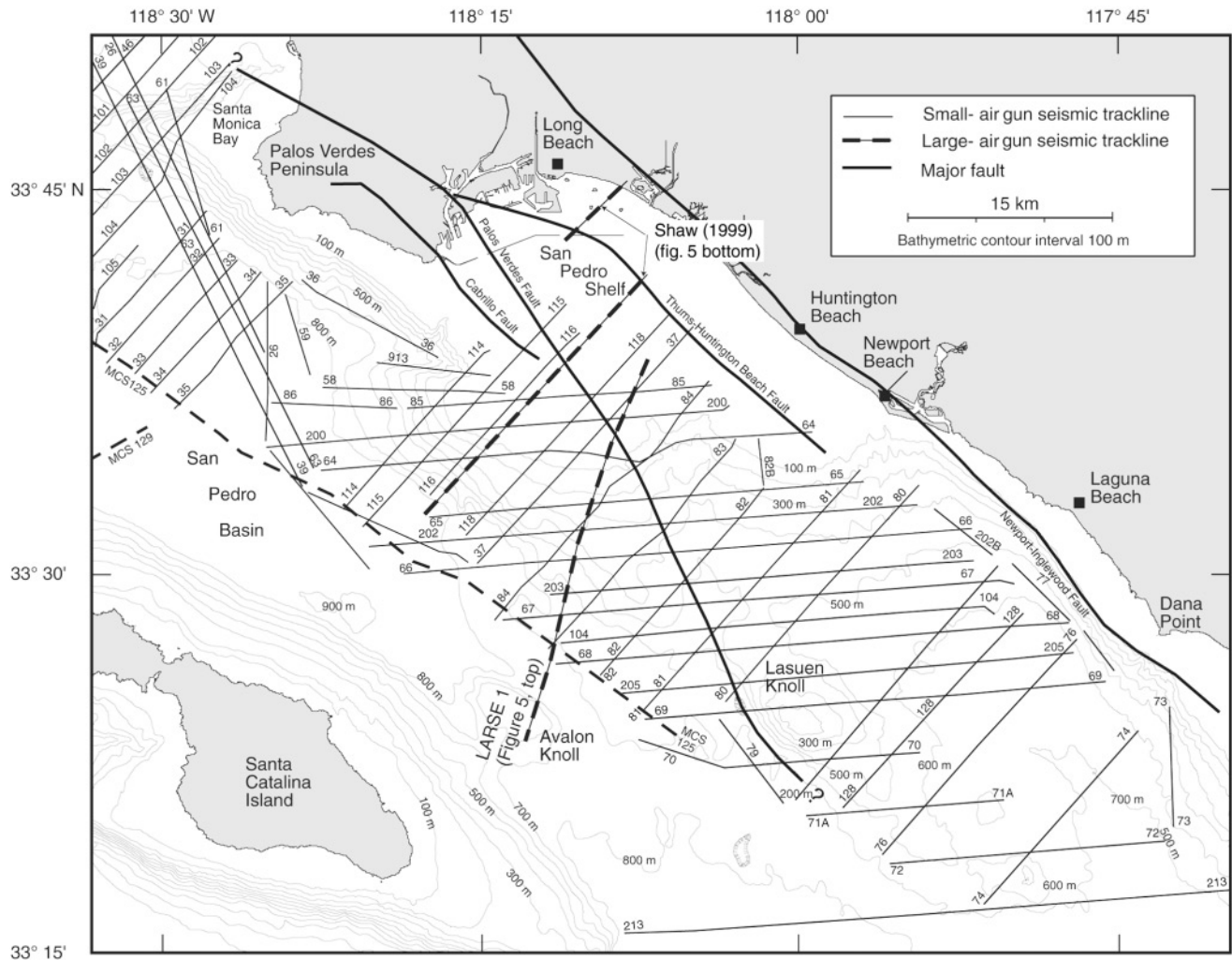


Figure 2. Tracklines of small airgun seismic-reflection data obtained during 1997–1998 by the USGS. These data were obtained with a 240-m-long streamer and with either a generator-injector airgun (each chamber was 35 in³) or a 40 in³ Bolt airgun. Location of LARSE 1 deep crustal seismic-reflection line is also shown (Brocher *et al.*, 1995). “MCS 125” and “MCS 129” indicate multichannel seismic-reflection data collected by the USGS during 1990.

Tectonic Evolution and Regional Geology

lines spaced 1.6 km apart. A magnetic high is located over the western San Pedro shelf, where seismic lines 115 and 200 intersect (Fig. 3, top). To help delineate the outline of the magnetic body (shown as a dashed line in both parts of Fig. 3), we used a computer algorithm to locate the maximum horizontal gradient of the magnetic field.

Offshore gravity values (Fig. 3, bottom) are from a 3-km grid of gravity measurements derived from scattered field data collected by the National Oceanic and Atmospheric Administration and the USGS and reduced to isostatic gravity values. These gravity data are accurate to several milligalileos, so they are suitable for regional but not detailed studies, and these data reveal mainly density variations within the middle and upper crust.

The study area includes the San Pedro continental shelf and the eastern part of the deep-water San Pedro basin, which lie west of the Los Angeles basin (Fig. 1), within the inner California Continental Borderland (CCB). During the early Miocene, lower crustal rocks were unroofed and exposed in wide areas of the CCB, when part of the Farallon oceanic plate that lay west of southern California stopped subducting and began to move northward with the Pacific plate (Nicholson *et al.*, 1994; Atwater and Stock, 1998). During this tectonism, regional oblique rifting and strike-slip deformation replaced margin-normal subduction. The resulting oblique extension of the continental margin is thought to have occurred simultaneously with the clockwise rotation of the Transverse Ranges (Luyendyk *et al.*, 1980;

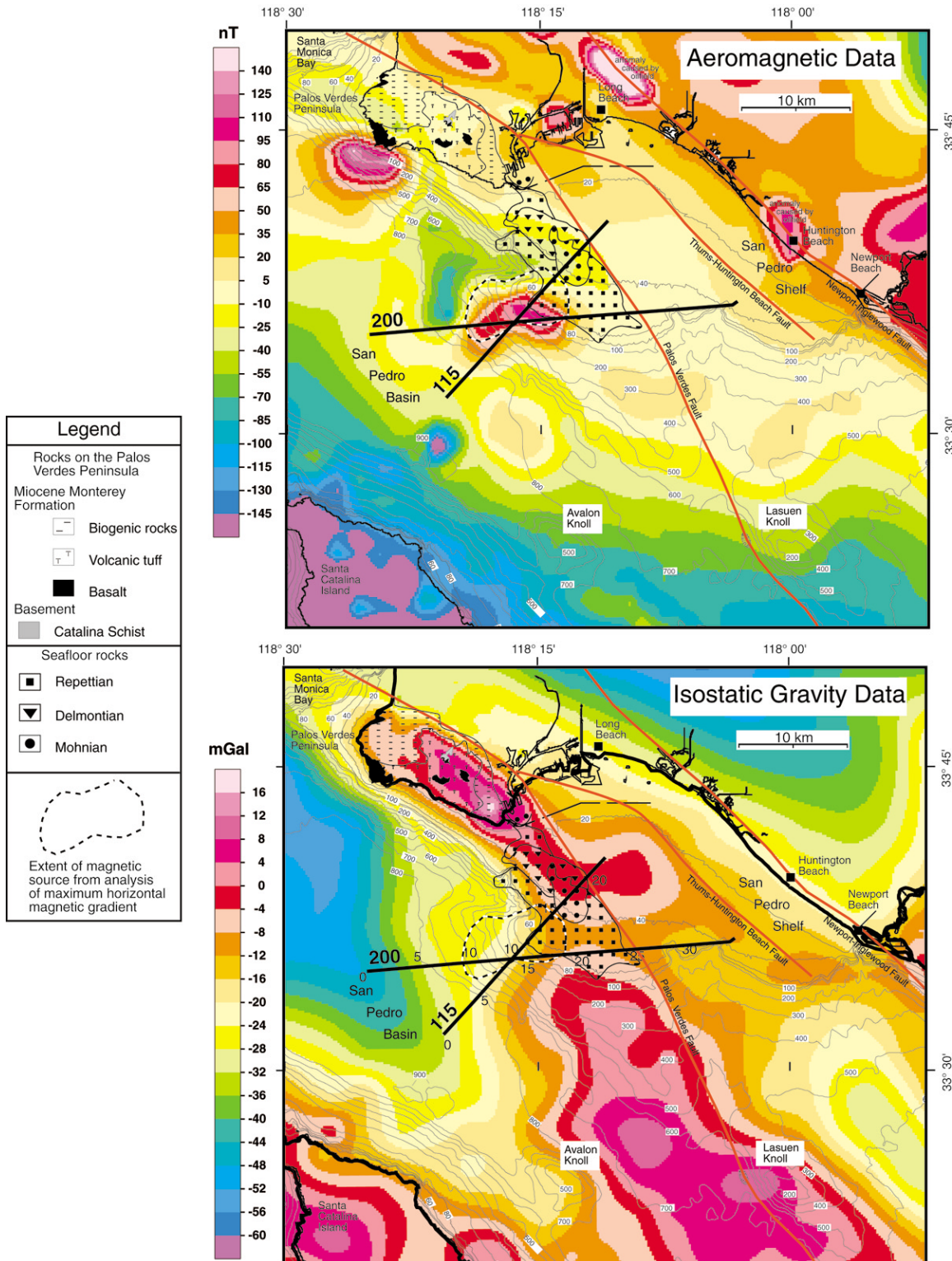


Figure 3. (Top) Aeromagnetic anomaly map of the study area. An aeromagnetic anomaly near the northwest corner of the Palos Verdes Peninsula occurs near an on-shore basalt outcrop, and a well within the outline of this anomaly penetrated thick Miocene basalt. Gravity and magnetic models of the isolated anomaly over the western San Pedro shelf are shown in Figure 2. Ages of seafloor rocks are from Nardin and Heney (1978). Onshore geology is from Woodring *et al.* (1946). (Bottom) Isostatic gravity map of the study area.

Kamerling and Luyendyk, 1985; Crouch and Suppe, 1993; Nicholson *et al.*, 1994). Blueschist- and amphibolite-facies metamorphic rocks from the former subduction zone were uplifted from lower-crustal depths and exposed at the surface. These rocks, which typically outcrop as the Catalina Schist, make up the basement complex beneath much of the inner CCB. Within the study area, this basement complex is buried beneath sedimentary rocks no older than Miocene. Middle Miocene volcanism that followed the crustal extension (Dickinson, 1997) produced pillow basalt and basalt sills exposed on the Palos Verdes Peninsula (Woodring *et al.*, 1946; Conrad and Ehlig, 1987; Stanley *et al.*, 2000) (Fig. 4).

In late Pliocene and Quaternary time, mainly the last 4 Ma, extensionally deformed rocks of the continental margin were involved in regional transpression (e.g., Wright, 1991; Crouch and Suppe, 1993). During the tectonic transition from extension to transpression, some middle Miocene normal and oblique-normal faults were reactivated as reverse and strike-slip faults (Rivero *et al.*, 2000). Blind thrust faults and fault-propagation folds also may have begun to form offshore and beneath the densely populated Los Angeles region (e.g., Namson and Davis, 1990; Shaw and Suppe, 1996). Near the San Pedro shelf, evidence for the Pliocene onset of this transpressive deformation comes from oil industry wells that penetrate the large Wilmington anticline. This anticline (axis shown in Fig. 1) deforms rocks northeast of the study area but did not exist prior to deposition of upper Miocene and lower Pliocene rocks (Olson, 1974). Transpressive folding of this anticline apparently was completed before the end of the late Pliocene (Truex, 1973).

Onshore Rocks

On the Palos Verdes Peninsula, metamorphic basement rocks are overlain with marked unconformity by a middle Miocene through Pliocene sedimentary succession that is similar to rock sequences encountered in offshore oil wells and revealed in MCS data (e.g., Fischer *et al.*, 1987; Wright, 1991). Under the peninsula, middle and late Miocene, deep marine rocks form a thick, heterogeneous sequence assigned to the Monterey Formation (Woodring *et al.*, 1946; Conrad and Ehlig, 1987; Barron and Isaacs, 2001) (Fig. 4). This formation includes not only cherty and phosphatic shale but also volcanic tuff and basalt. The volcanic rocks have been dated to between 15 and 14 Ma (Conrad and Ehlig, 1987; Henry, 1987; Stanley *et al.*, 2000). Lower Pliocene rocks on the Palos Verdes Peninsula unconformably overlie the Monterey Formation, and upper Pliocene rocks are absent.

Rocks under the Palos Verdes Peninsula have long attracted the attention of geologists because rapid uplift during Quaternary time caused an impressive flight of wave-cut terraces to develop (Woodring *et al.*, 1946; Bryan, 1987; Ward and Valensise, 1994). A concern of seismologists is that this intense deformation extends south of the Palos Verdes Peninsula to involve offshore faults. This possibility has been difficult to evaluate, given the generally featureless mor-

phology of the San Pedro shelf, which is broad, flat, and shallow, most of it is less than 50 m deep (Fig. 1).

Age of Offshore Rocks

The offshore stratigraphy is known primarily from oil industry coring and drilling. Numerous shallow cores, obtained south of the Palos Verdes Peninsula and west of the Palos Verdes fault zone, show that middle Miocene through Pliocene rocks are exposed at the seafloor in a southeast-trending zone near the shelf break (Nardin and Henyey, 1978) (Fig. 4). These seafloor rocks cause high backscatter in multibeam bathymetric data. Seismic-reflection data obtained over these outcrops show that reflections from Miocene and Pliocene rocks are distinctively parallel and continuous over long distances (10–20 km).

Other information concerning the age of offshore rocks comes from geologic cross sections based on well data from the Beta oil field (Henry [1987]; figure 13 of Wright [1991]). Comparison of one cross section (Wright [1991], cross section location shown Fig. 4) to depth-converted, USGS seismic-reflection data (Fig. 5) reveals not only the probable thickness and age of rocks on opposite sides of the Palos Verdes fault zone, but also the depth to crystalline basement on the west side of the fault. The comparison indicates that, near the Beta oil field and west of the Palos Verdes fault zone, Quaternary sediment is thin or absent and that Miocene and Pliocene rocks are exposed at the seafloor. This exposure agrees with findings from the shallow coring mentioned earlier. East of the Palos Verdes fault zone, however, late Pliocene and Quaternary rocks and sediment aggregate in thickness to as much as 1.5 km.

Depth to Offshore Metamorphic Basement

In general, reflections from the top of metamorphic basement are not apparent in small airgun, seismic-reflection data described here, but evidence from rock outcrop, oil industry operations, and seismic-refraction data all indicate that this basement lies at relatively shallow depth (<3 km) beneath the shelf and slope.

Regionally, the depth to basement decreases westward from within the Los Angeles basin toward the offshore study area, and basement deepens offshore, southeastward from its crop out on the Palos Verdes Peninsula (e.g., Olson, 1974; Fischer *et al.*, 1987; Wright, 1991). This configuration is demonstrated primarily by information compiled from oil industry sources. For example, regional cross sections by several authors indicate that east of the Palos Verdes fault zone and Peninsula, the top of basement is mainly 1–1.5 km deep (sections 5 and 12 of Davis and Namson [2002]; locations shown in Fig. 4). The top of basement deepens southeastward into the offshore area to a depth of about 3 km.

Another regional cross section, constructed in part from depth-converted seismic-reflection data (Shaw, 1999) (summarized in Fig. 5, bottom; section location shown in Fig. 2), indicates that basement rocks below the coast southwest of

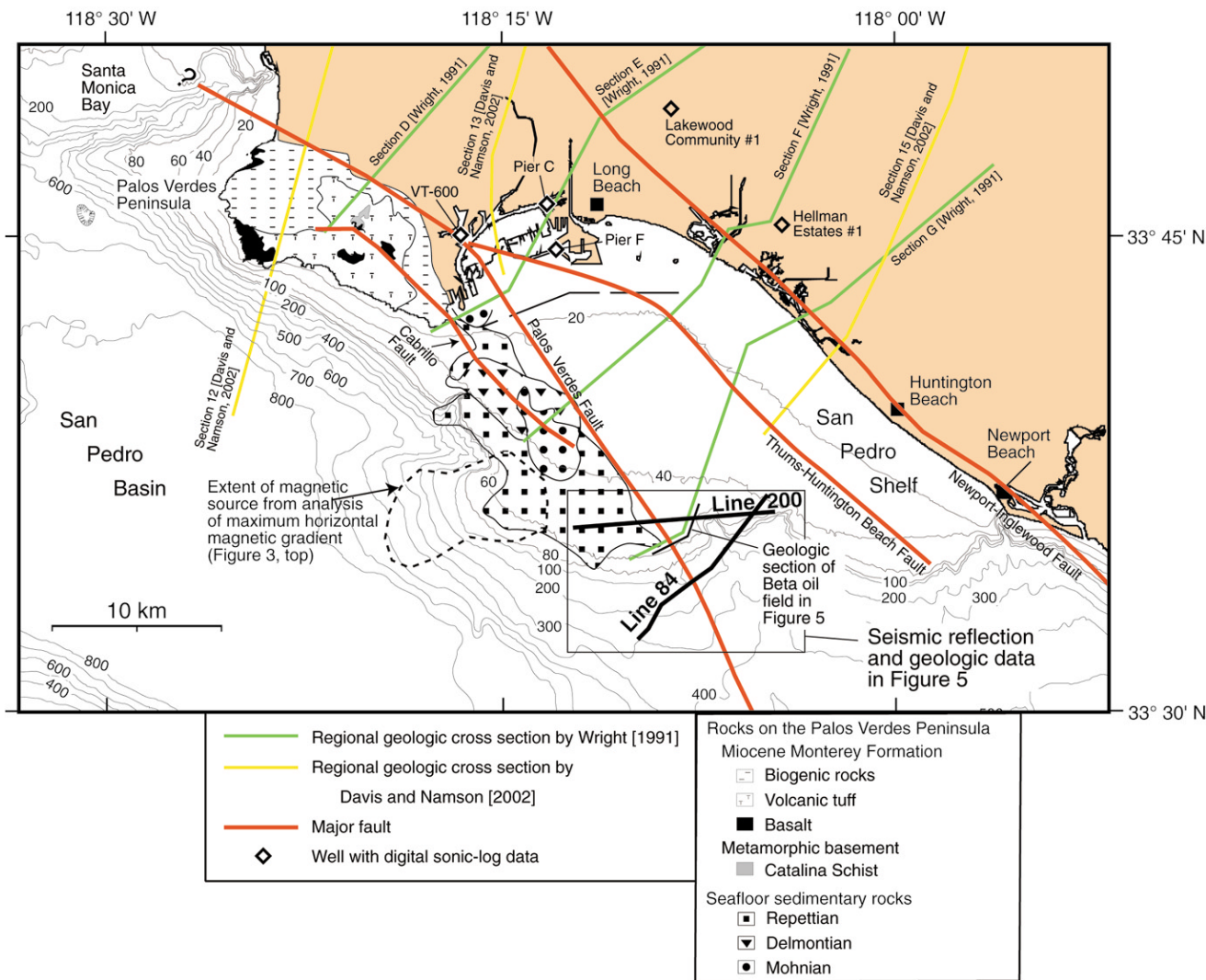


Figure 4. Locations of regional cross-sections compiled by various authors and discussed in the text. A cross section through the Beta oil field (Wright, 1991) shows the approximate age of basin fill in Figure 5. Biostratigraphic data from strata exposed at the seafloor are from Nardin and Henyey (1978). Onshore geology of the Palos Verdes Peninsula is from Woodring *et al.* (1946).

the Newport–Inglewood fault were encountered in a well at about 3-km depth. A cross section through the Beta oil field (figure 13 in Wright [1991]) provides the only direct information we have on basement depth southwest of the Palos Verdes fault zone, where an oil well encountered basement rocks at about 2.5 km depth (Fig. 5).

Basement depth determined from drilling in the Beta field compares favorably to the depth estimated from tomographic analysis of wide-angle seismic data collected during the LARSE experiment (ten Brink *et al.*, 2000) (location of LARSE 1 seismic-reflection line shown in Fig. 2). Assuming that rock velocities exceeding 5 km/sec indicate acoustic basement, either volcanic or metamorphic rock, then northeast of the Palos Verdes fault zone, basement is 2.5–3 km deep, and southwest of this fault zone, basement is about 2.5 km deep and deepens to the southwest.

Previous Findings about the Main Offshore Structures

The major offshore faults include the Newport–Inglewood, Thums–Huntington Beach, and Palos Verdes fault zones (Fig. 1). The Newport–Inglewood fault exhibits right-lateral strike-slip motion and either forms the contact between different basement types or closely follows this contact (Barrows, 1974; Wright, 1991; Bohannon and Geist, 1998). North and east of this fault, basement rocks consist of Jurassic and Cretaceous crystalline continental crust, typical of the Peninsular Ranges, whereas south and west of the fault, the basement is Catalina Schist. The 1933 Long Beach earthquake (M_w 6.4) probably occurred along the Newport–Inglewood fault (Hauksson and Gross, 1991) and was the largest recorded earthquake to have struck near the coast.

The Thums–Huntington Beach fault splays southeast-

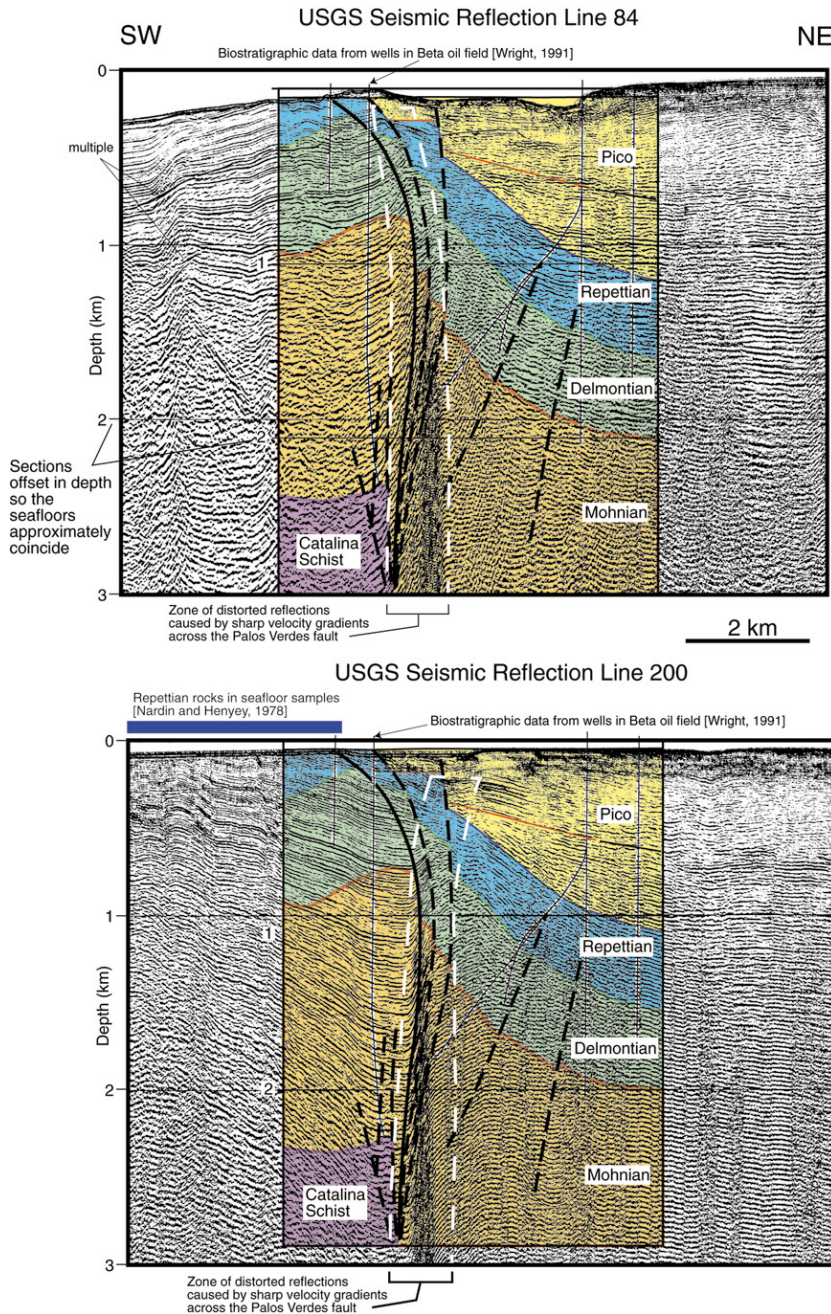


Figure 5. Comparison of depth-converted seismic-reflection data from this study with stratigraphic information from the Beta oil field (Wright, 1991). Rocks west of the Palos Verdes fault zone are mainly Miocene and Pliocene in age, whereas thick late Pliocene and Quaternary rocks and sediment lie on this fault zone's east side.

ward away from the Palos Verdes fault zone (Wright, 1991) (Fig. 1). Interpretive cross sections differ on fundamental issues about this fault in that one shows a normal fault that dips east and is downthrown on the east (Wright, 1991); another section shows that it dips west and is downthrown on the west and merges downward with the Palos Verdes fault zone (Davis and Namson, 2002).

The Palos Verdes fault zone has been postulated to extend southeastward from the northern part of Santa Monica Bay and to continue southwest of Lasuen Knoll (e.g., Greene and Kennedy, 1987; Legg *et al.*, 1991; Wright, 1991) (Fig. 1). Although the Palos Verdes fault zone has been postulated to end in the northwest below northern Santa Monica

Bay, no indication of a recently active part of this fault has been observed in high-resolution seismic-reflection data collected in the southern part of this bay (Nardin and Henyey, 1978; Fisher *et al.*, 2003). Where the Palos Verdes fault zone passes northeast of the Palos Verdes Peninsula, the total fault-slip rate appears to be around 3 mm/yr, based on analysis of wave-cut terraces and offset stream courses (Ward and Valensise, 1994; McNeilan *et al.*, 1996). McNeilan *et al.* (1996) proposed that in the recent past, the main style of movement along the Palos Verdes fault zone has been strike slip. Multibeam bathymetric data show recent scarps along this fault near Lasuen Knoll (Marlow *et al.*, 2000).

The geometry of the Palos Verdes fault zone at depth is

not well characterized. Davis and Namson (2002) depicted this fault zone with a steep southwestern dip (about 60°) in the upper 5 km of the crust, and below 7 km, the dip was proposed to shallow to about 25° southwest. Similarly, Shaw (1999) indicated that the Palos Verdes fault zone is steep to vertical in the upper 5 km of the crust, and at greater depth, the fault dips about 30° southwest (Fig. 6, bottom). A stack of LARSE MCS data shows a similar west-dipping fault geometry (Fig. 6, top). However, cross sections by Wright (1991) depict the Palos Verdes fault zone as a vertical or steeply east-dipping, strike-slip fault, at least for depths shallower than about 9 km.

Offshore Structure from Seismic-Reflection Data

To facilitate discussion, we divide the study area into two structural belts that are separated by the Palos Verdes fault zone. The eastern belt includes the Wilmington graben (Fig. 1), which includes a thick (1–2 km) section of Quaternary rocks and sediment. The western structural belt includes variably deformed, primarily Miocene and Pliocene rocks that lie west of the Palos Verdes fault zone.

Structural Belt East of the Palos Verdes Fault Zone: The Wilmington Graben

The eastern belt includes the Wilmington graben, which is an elongate, nearshore basin confined between the Newport–Inglewood and Palos Verdes fault zones (Fig. 1). (The term “Wilmington graben” [Fischer *et al.*, 1987] is somewhat misleading because the graben is bounded by what are probably strike-slip, not normal, faults. Even so, we use this term because of its precedence in the literature and common usage.) The Thums–Huntington Beach fault deforms rocks within the graben (Fig. 2). Unfortunately, owing to environmental restrictions placed on our surveys, none of our seismic-reflection lines crosses this fault. However, geologic cross sections published elsewhere show this fault’s structure (see section locations in Fig. 4). For example, Wright (1991) showed that the northeast side of this fault dropped down, forming the large Wilmington anticline.

Rocks within the Wilmington graben are only mildly deformed, except in the far western part of the graben, directly adjacent to the Palos Verdes fault zone (Fig. 7; location shown in Fig. 2). Seismic-reflection data indicate that very shallow strata within the graben are subhorizontal and overlie a shallow unconformity (at a travel time of about 0.2 sec), but this relationship is largely obscured by water-bottom multiples. This unconformity and the uppermost part of the section in the Wilmington graben are deformed by and extend cross the Palos Verdes fault zone, indicating relatively recent fault movement. The unconformity truncates the tops of underlying beds that have an apparent southwest dip. Down to a travel time of about 0.8 sec (about 800-m depth), a deltaic sequence progrades across the graben in an apparent southwestward direction. A reverse fault within the graben (Fig. 7; below shotpoint [SP] 1500) offsets this unconformity but does not extend far upward through the over-

lying rocks. A third unconformity is evident on the right half of Figure 7, at a travel time of 1.5 sec.

The Wilmington graben ends to the southeast along the east-striking part of the continental slope that delimits the San Pedro shelf (Fig. 2). This graben probably ends below the east-striking part of the continental slope that bounds the San Pedro shelf on the southeast. However, our MCS data do not reveal the structure where the graben ends. In the far southeastern part of the study area, east of Lasuen Knoll, the Newport–Inglewood fault and the Palos Verdes fault zone diverge, and the widening deep-water area between these faults has received extensive and thick turbidite fill from channels that make up the Newport Canyon.

Structural Variation along the Palos Verdes Fault Zone

The Palos Verdes fault zone is the most prominent and arguably the most complicated structure revealed by our seismic-reflection data. The fault zone separates the folded shelf rocks, primarily of Miocene and Pliocene age, that occur west of the Palos Verdes fault zone (Nardin and Henyey, 1978) from a thick (1-km typical) section of mainly flat-lying upper Pliocene and Quaternary rocks and sediment along the fault’s east side (Fig. 5).

Cross sections (locations shown in Fig. 4) indicate that at shallow depth (<1 km) under the San Pedro shelf, the Palos Verdes fault zone is nearly vertical but that it curves downward to dip steeply west. This west dip is also evident in a stack of MCS reflection data obtained along LARSE line 1 (Fig. 6, top). MCS data in Shaw (1999) (Fig. 6, bottom) depict this fault zone with a west dip and indicate that rocks below about 1 km depth along the west side of the fault dip east and terminate against the fault plane.

Small airgun, seismic-reflection data (Plate 1 [unbound insert to this issue]) reveal that at shallow depth (<1 km) under the northern San Pedro shelf, the Palos Verdes fault zone dips steeply west or is vertical (Plate 1, seismic-reflection sections 115 and 118). Also shallow strata within the Wilmington graben extend westward through the Palos Verdes fault zone, are offset by the fault strands, and appear to overlie unconformably Miocene and Pliocene rocks on the fault’s west side.

The intensity of compressional deformation decreases southeastward across the San Pedro shelf. In particular, the anticline along the west side of the fault zone (Plate 1; seismic section 115) decreases in structural relief and broadens southeastward (Plate 1; seismic section 118). Southeast of the shelf, below the upper part of the slope, this anticline dies out entirely, as little trace of it appears on seismic section 84 (Plate 1). In fact, this section shows that faults along the projected location of the Palos Verdes fault zone all exhibit normal separation. Such faults are more readily evident on seismic-reflection section 66 (Plate 1), where the main fault strands dip east.

A bathymetric saddle, where the seafloor attains a depth as great as 500 m, separates the southeastern edge of the San

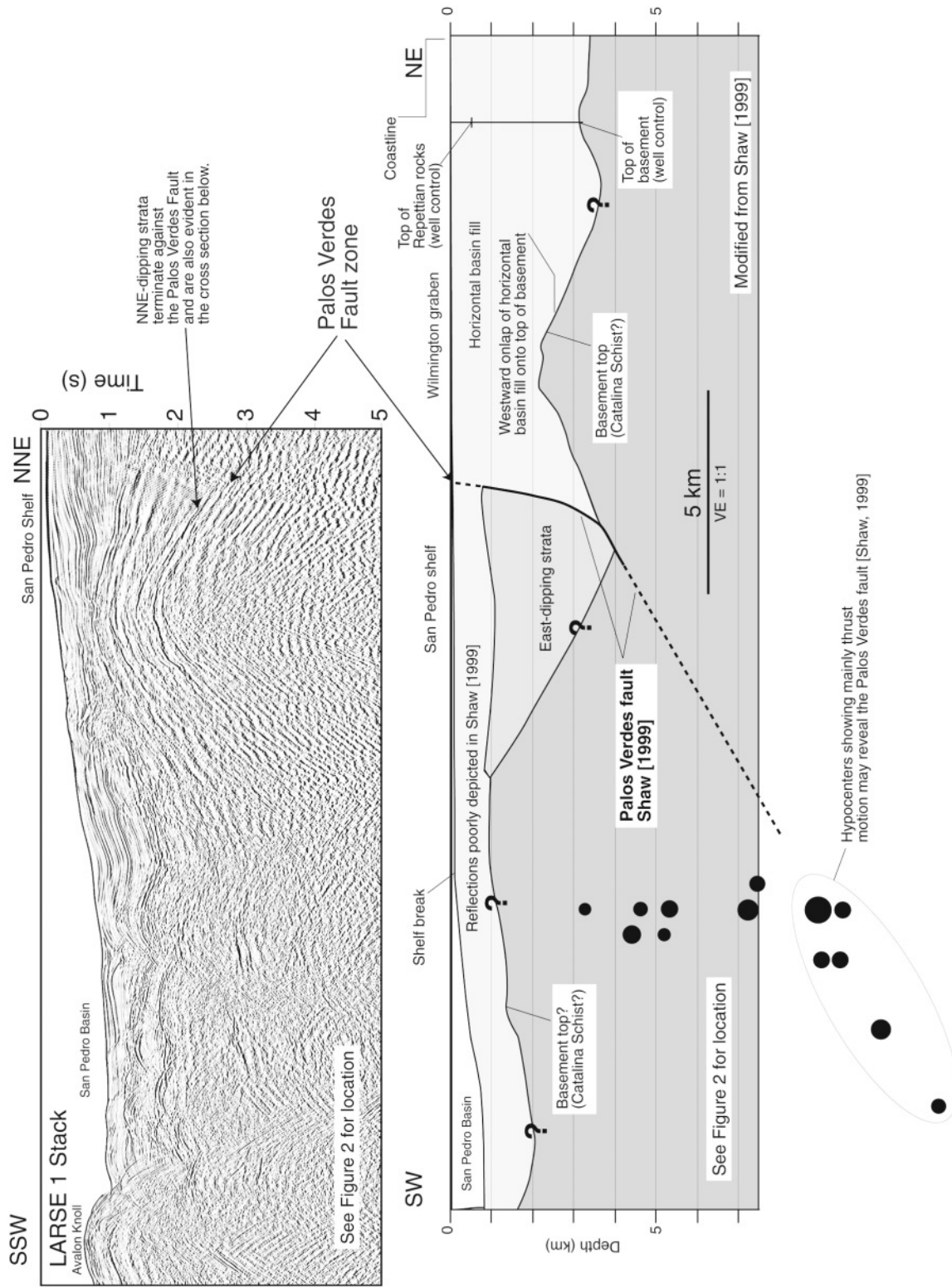


Figure 6. (Top) Stack of LARSE line 1, deep-crustal, seismic-reflection (Brocher *et al.*, 1995) data obtained across the San Pedro shelf and the Palos Verdes fault zone (seismic line location shown in Fig. 2). These data show that the fault zone dips west at large travel times. (Bottom) A simplified view of the composite cross section by Shaw (1999) (location shown in Fig. 3 top), which shows one interpretation of the deep-crustal structure of the Palos Verdes fault zone.

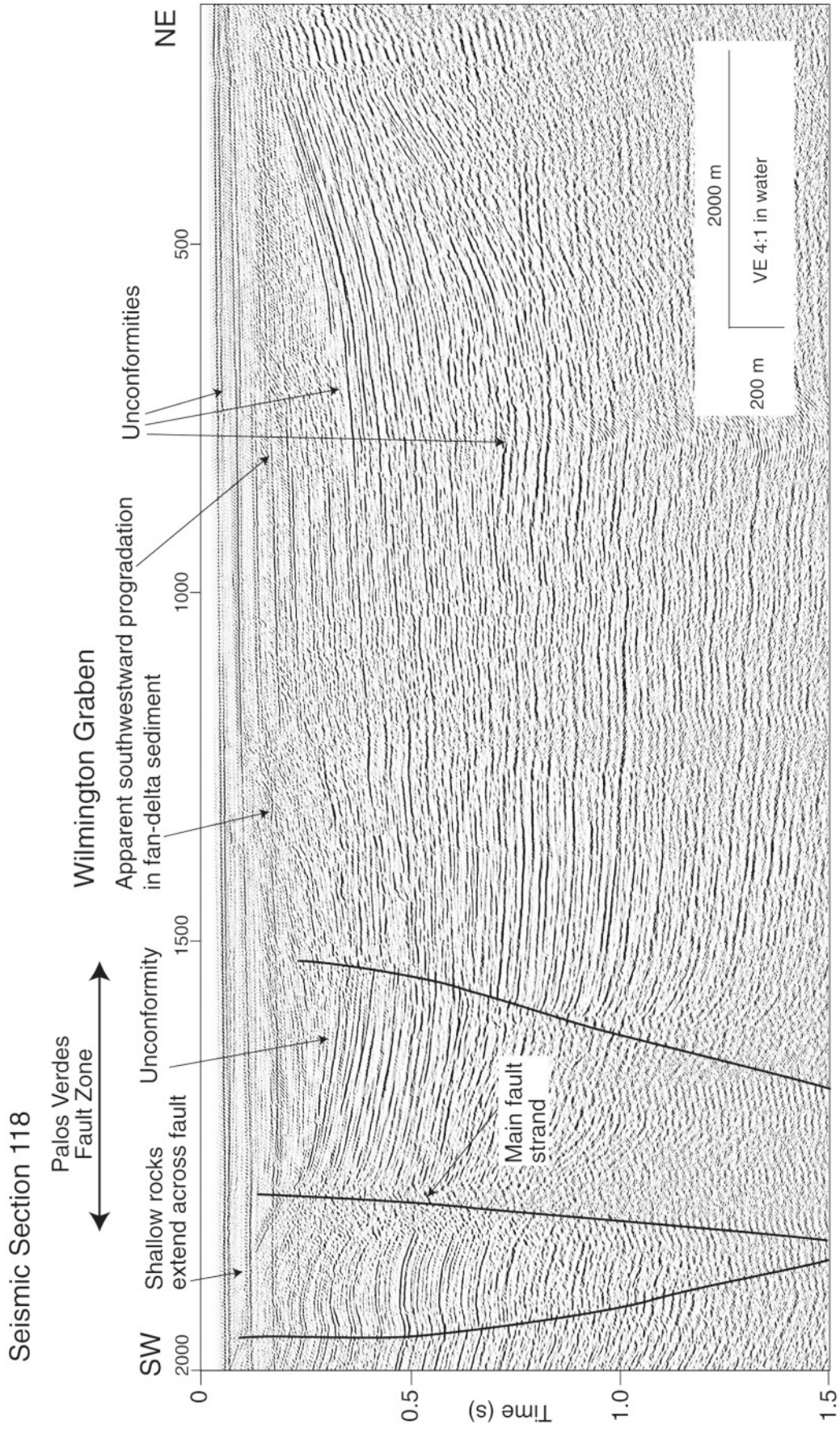


Figure 7. Seismic section over the Palos Verdes fault zone and Wilmington graben under the San Pedro shelf. Section location is shown in Figure 2.

Pedro shelf from the high-standing Lasuen Knoll (bathymetric contours shown in Fig. 1 and the index map in Plate 1). An oblique view of multibeam bathymetric data obtained over the San Pedro shelf and slope (Fig. 8) shows the incised head of the San Gabriel Canyon at the southeastern edge of the San Pedro shelf. This channel head is located where underlying rocks are deformed by normal faults that make up the Palos Verdes fault zone, suggesting that the extensional deformation helped determine the course of the channel's upper reach. The San Gabriel Canyon crosses the Palos Verdes fault zone at a highly oblique angle, and this channel is not obviously deflected, either horizontally or vertically. This channel, however, does bifurcate near this crossing:

One channel branch extends southeastward along the west scarp of the Lasuen Knoll, following the Palos Verdes fault zone (Marlow *et al.*, 2000). The other channel branch veers southwest across the floor of the San Pedro basin.

The bathymetric saddle marks an important structural transition along the Palos Verdes fault zone, because south-eastward through the saddle both the dip and the vergence direction of the fault zone change. The sequence of seismic sections 67, 81, and 80 (Plate 1) shows that near Lasuen Knoll, this fault zone exhibits reverse separation and dips east, which is opposite to the west dip of the fault under the northern San Pedro shelf. This east dip is apparent on seismic section 67. The dip change of the Palos Verdes fault

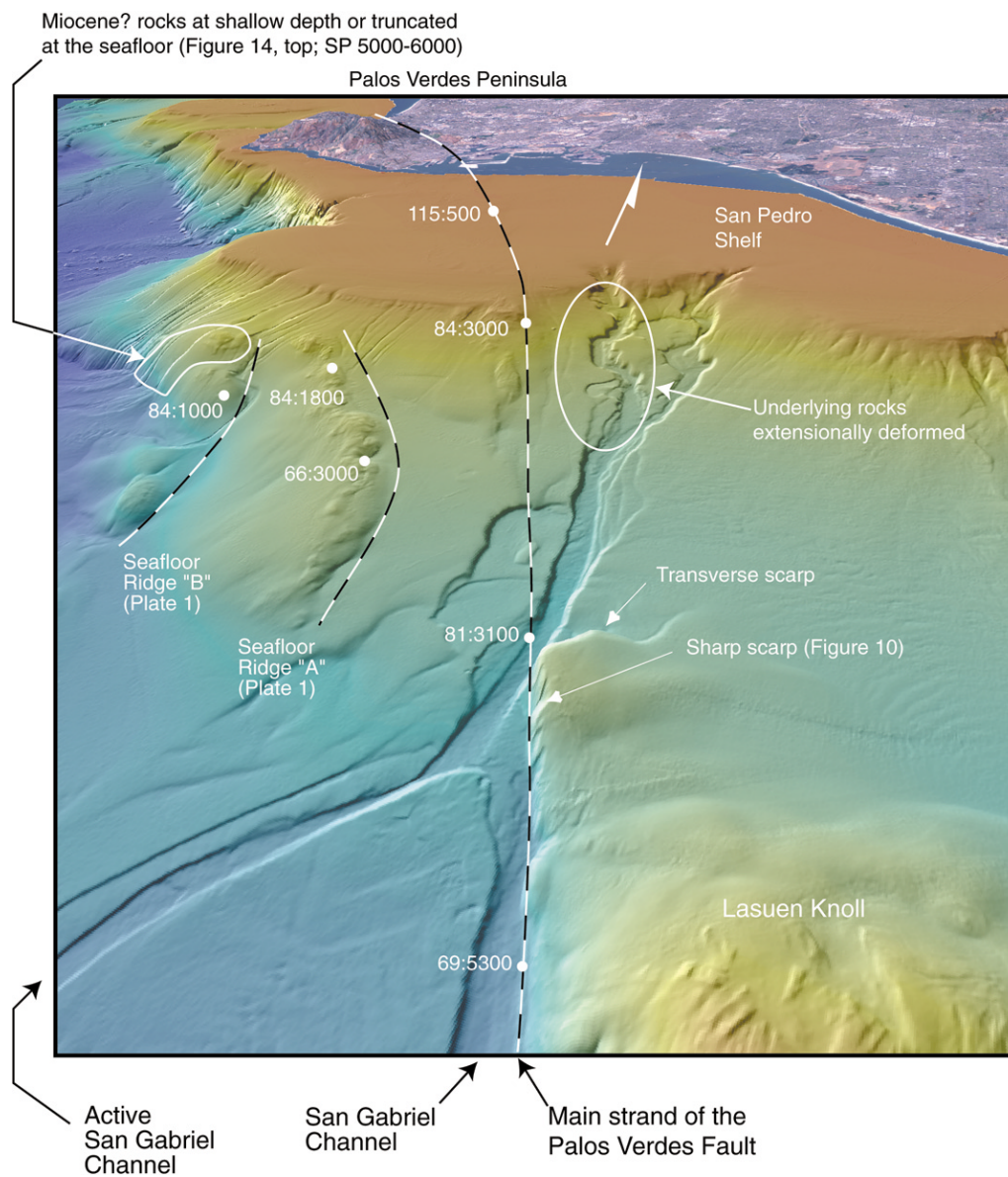


Figure 8. Oblique view to the northwest of multibeam bathymetric data over the San Pedro shelf and Lasuen Knoll (Gardner and Dartnell, 2002). Annotation on the figure such as “84:1800” refers to seismic section 84, SP 1800 on Plate 1. Dashed lines show interpreted faults.

zone occurs under the bathymetric saddle and possibly under the zone of normal faults described earlier.

Seismic section 66 (Plate 1) shows that rocks within the Wilmington graben flex upward along a short-radius fold that clearly does not include shallow faulting. However, faulting becomes progressively more apparent southeastward along the east boundary of the dipping rocks. For example, kink bands clearly evident on seismic section 67 (Plate 1 and Fig. 9; below SPs 4000 and 4300) reveal topography on the plane of an underlying, east-dipping thrust fault. The underlying fault lies below the depth of penetration of our seismic-reflection data; even so, we interpret this fault to be the Palos Verdes fault zone.

Clear faulting along the east flank of the dipping rock section is shown by seismic section 80 (Plate 1, below SP 1500), where the dip change occurs along a west-dipping fault, showing reverse separation, that offsets very shallow sediment and perhaps the seafloor. The increased intensity of faulting along this zone to the southeast mirrors the heightened bathymetric expression of the knoll.

A shallow unconformity that truncates east-dipping rocks in the Wilmington graben (Fig. 9) crosses the Palos Verdes fault zone. Strongly but irregularly reflective strata reveal coarse deposits, probably channel-fill and (or) lobe deposits, within the San Gabriel turbidite system that overlie this unconformity. Complex reflections from these deposits foiled our attempt to determine whether or not the unconformity extends unbroken across the Palos Verdes fault zone. However, between SPs 4000 and 4200 (Fig. 9), east-dipping rocks under the unconformity are parallel bedded and dip east; in contrast, strata above the unconformity are flat lying. These relationships suggest that along the Palos Verdes fault zone near the north part of Lasuen Knoll, eastward tilting ended before the erosion that cut the unconformity. Significantly, tilting has not resumed since the erosion, because the turbidite channels of the San Gabriel Canyon have not been shifted away from what was once the locus of uplift and tilting (Fig. 8). Hence, the vertical component of deformation ended before the unconformity's cutting and the later establishment of the modern turbidite system.

A somewhat different picture of the deformation history is revealed by seismic section 68 (Fig. 10), which crosses the Palos Verdes fault zone close to Lasuen Knoll (location shown in Fig. 2). This seismic section shows a sharp seafloor scarp that is perched above and west of an anticline and an east-dipping fault (below SP 2500). These structures lie along the Palos Verdes fault zone, and following Marlow *et al.* (2000), we propose that they are the southeastward extension of this fault zone along the west flank of Lasuen Knoll. The seafloor scarp associated with the Palos Verdes fault zone (Fig. 10) is clearly evident in the oblique views of multibeam bathymetric data (Fig. 8, labeled "sharp scarp"). Other multibeam bathymetric data show this scarp has sharp edges that contrast strongly with the rounded contours of the seafloor elsewhere. On this basis, the scarp appears to be young. Taken together, seismic-reflection and multibeam

bathymetric data show that the Palos Verdes fault zone near Lasuen Knoll exhibits reverse separation and dips east. Furthermore, this part of the fault zone has been active recently.

An unconformity (indicated by an arrow below SP 3200 on Fig. 10) separates rocks below, which have constant thickness, from sediment above, which thins westward. Sediment just above the unconformity thins gradually westward, whereas beds higher up in the section thin more sharply. The geometry of these strata indicates that broad eastward tilting of the upper plate of the Palos Verdes fault zone began shortly after the unconformity was cut and buried.

An anticline underlies the seafloor scarp along the east side of the Palos Verdes fault zone (Fig. 10, below SP 2500), and the anticline dies out upward through the rock section, so that shallow rocks are barely arched. Likewise, a minor fault east of the anticline, below SP 2700, offsets deep basin rocks and extends upward through the unconformity but dies out just above the unconformity. A minor anticline (below SP 3000) also dies out upward. All of these structures indicate that through time near the knoll, folding and faulting focused along the Palos Verdes fault zone decreased in intensity to be replaced by regional tilting.

East-dipping rocks under the crest of Lasuen Knoll are truncated at the seafloor, and this truncation may have occurred subaerially, as suggested by a modified version of seismic section 69 (Fig. 11). To make this figure, the seismic section was rotated 3° counterclockwise so that discontinuous, flat parts of the knoll's crest as well as notches in the seafloor can be connected by dashed horizontal lines. We propose that these lines connect wave-cut platforms and terraces. This interpretation is bolstered by the recovery of a shelf-edge benthic fauna from a piston core obtained under deep water (373 m) along the knoll's flank; this fauna does not appear to have been displaced (M. McGann, personal comm., 2003). This finding is consistent with our proposal that the terraces were cut at sea level. The youth of submergence derived from fossil evidence agrees with the conclusion we drew earlier about the youth of the tilting of rocks along the west side of the Wilmington graben.

A point we emphasize is that the sharpness of the seafloor scarp ("sharp scarp" in Fig. 8) indicates that the Palos Verdes fault zone was reactivated recently and is most likely responsible for the eastward tilting of rocks in the Wilmington graben and under Lasuen Knoll. The style of deformation that involves broad tilting differs from the folding and faulting that preceded the erosion that produced the unconformity. This older deformation appears to have been local to the fault zone.

A scarp transverse (labeled in Fig. 8) to Lasuen Knoll has sharp edges and is nearly perpendicular to the Palos Verdes fault zone. This scarp marks the beginning of the sharp scarp that for nearly 30 km extends along the foot of the Lasuen Knoll and marks the location of the Palos Verdes fault zone. We propose that a fault underlies the transverse scarp and that it played a key role in the recent uplift of Lasuen Knoll.

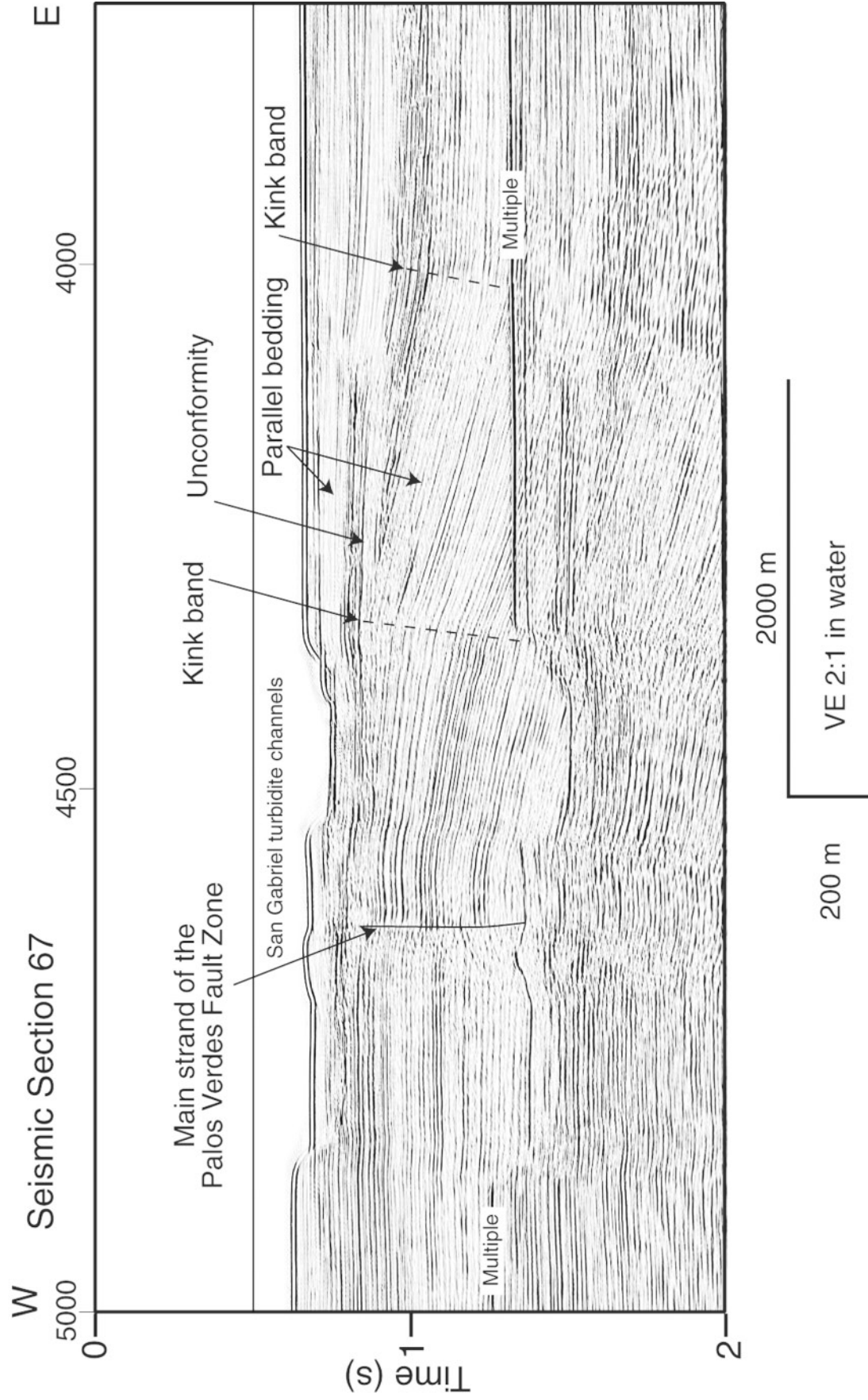


Figure 9. Detailed seismic section 67 over the Palos Verdes fault zone under the bathymetric saddle between the San Pedro shelf and the Lasuen Knoll. Section location is shown in Figure 7. Recent vertical movement along the main fault strand seems to have been small because the San Gabriel Canyon cuts into the fault's upper plate.

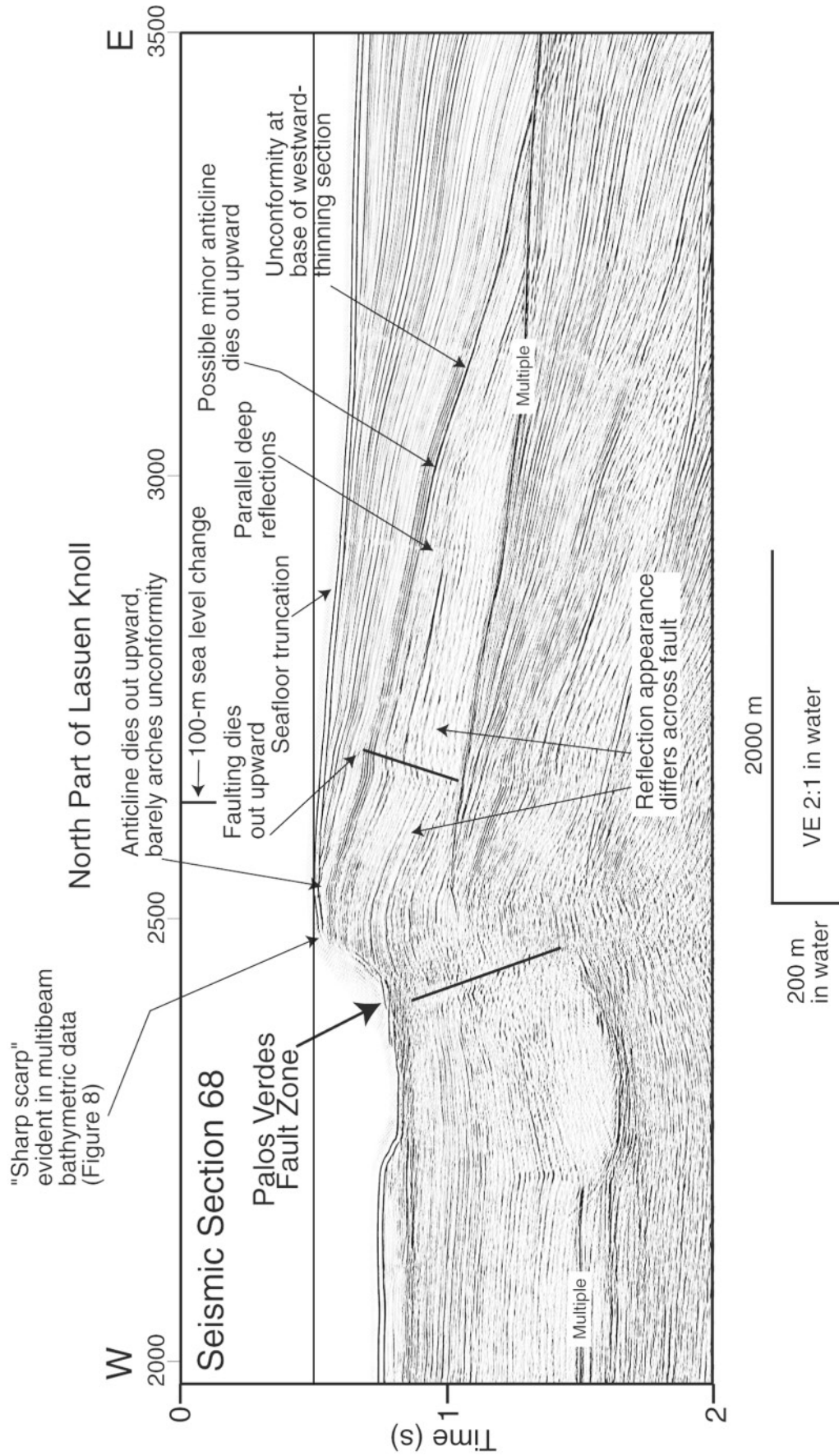


Figure 10. Detailed seismic section 68 over the Palos Verdes fault zone and Lasuen Knoll, showing the stratigraphy and structure of the “sharp scarp” that is also annotated in display of multibeam bathymetric data (Fig. 11). Section location is shown in Figure 7.

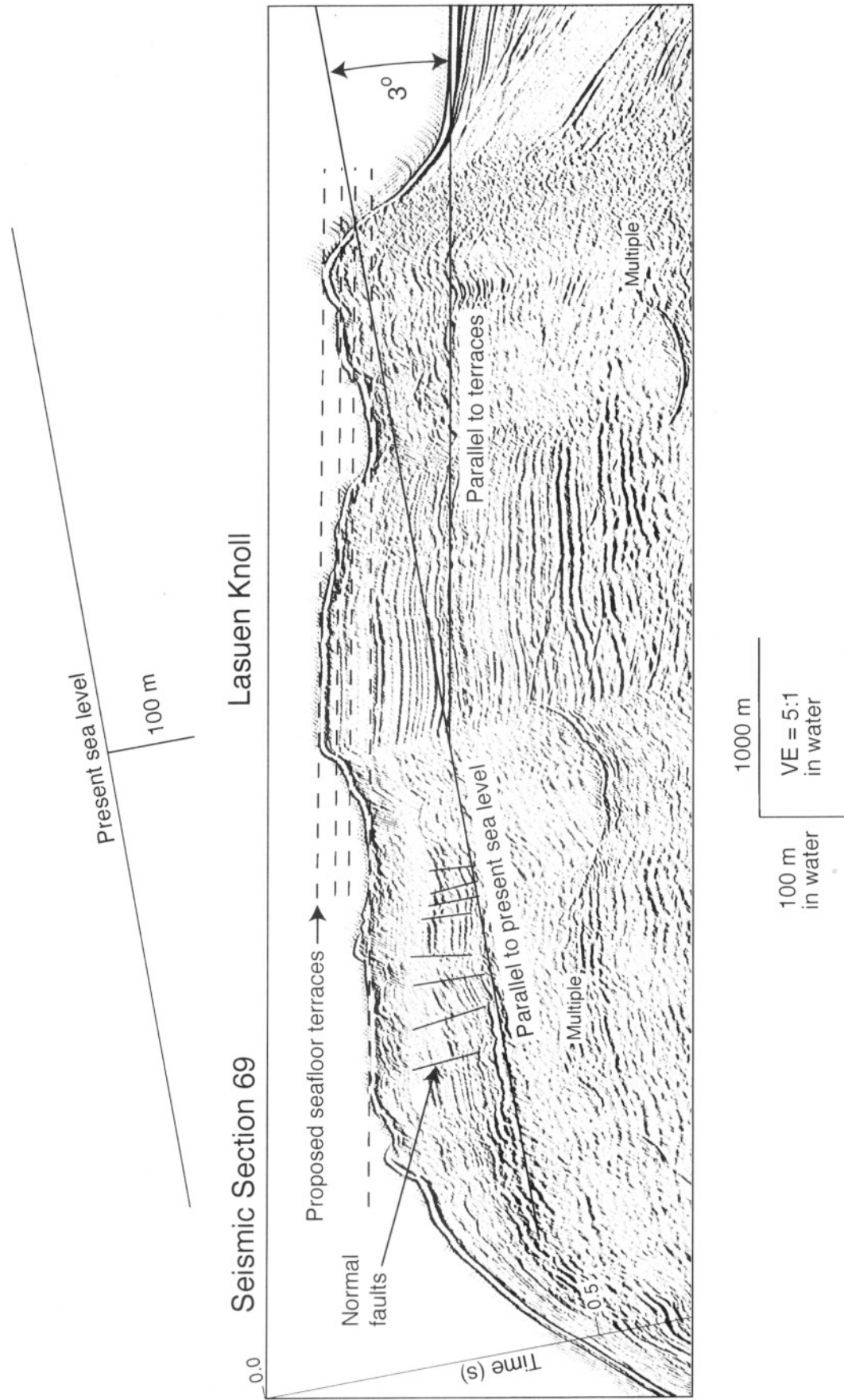


Figure 11. Detailed seismic section 69 from near the crest of Lasuen Knoll, showing inferred wave-cut terraces. The seismic section is vertically exaggerated and has been rotated counterclockwise by 10°, which corresponds to a 3° rotation in natural coordinates, as annotated on the section. Section location is shown in Figure 7.

Southeast of the crest of Lasuen Knoll (seismic sections 69 and 70 on Plate 1), deep rocks on the west side of the Palos Verdes fault zone are faulted and folded. Younger rocks onlap these deep, deformed rocks with sharp angularity. The dip of the Palos Verdes fault zone in the area of seismic sections 69 and 70 is ambiguous owing to complex rock structure, but the fault appears to be steep. The fault zone is about 1 km wide and includes at least four fault strands.

Poorly reflective rocks make up the west part of the fault's upper plate. This loss of reflectivity could be due to high strain along closely spaced faults. Another possibility is that the poor reflectivity indicates an ancient landslide.

The Palos Verdes fault zone is difficult to trace southeast of the Lasuen Knoll, mainly because seismic lines are widely spaced, but also the geologic structure is less distinct than farther northwest. Seismic section 213 (Plate 1), for example, shows only subdued seafloor and structural relief, and reflections indicate several candidate features that could be the fault zone's southeastward extension. On the basis of the eastward curve of bathymetric contours that outline the Lasuen Knoll between seismic lines 70 and 213 (index map to Plate 1), the Palos Verdes fault zone might intersect seismic-reflection line 213 between SPs 5000 and 6000. Another possibility is that motion along the Palos Verdes fault zone is transferred onto several fault splays southeast of the knoll.

Structural Belt West of the Palos Verdes Fault Zone

The western structural belt includes rocks west of the Palos Verdes fault zone and under the western San Pedro shelf as well as those below the slope and within the deep-water San Pedro Basin (Fig. 1). The western belt harbors much evidence for strong deformation and active tectonics. For example, the floor of the San Pedro Sea Valley, a deep notch cut southwestward into the shelf edge, is covered by debris from recent submarine landslides. Furthermore, the main geologic structures in the western belt include a large anticline and syncline (see Figs. 12 and 13) that border the Palos Verdes fault zone on the west.

The subslope anticline increases in structural relief northwestward beneath the San Pedro shelf. Projecting this anticline's axis (Fig. 12) northwestward along the strike indicates that this axis would traverse the area where Miocene and Pliocene rocks crop out at the seafloor (Nardin and Henyey, 1978) (Fig. 4). In addition, the projected axis would merge with the trend of the high topographic elevation of the Palos Verdes Peninsula.

The axis of the syncline under the west part of the San Pedro shelf (Fig. 12) can be extended northwestward to continue along the axis of the San Pedro Sea Valley. This connection strongly suggests that the sea valley's location was controlled by the synclinal structure of underlying rocks. The walls of this valley, especially the north wall, are known to have spawned one or more submarine landslides (e.g., Locat and Lee, 2002). A debris avalanche that is 14 km long and partly fills the San Pedro Sea Valley occurred about

7500 years ago is much larger than more recent failures (Normark *et al.*, 2002). The dips of rocks along both sea valley walls are toward the colinear axes of the syncline and sea valley. This inward dip probably explains why landslides were more commonly shed here than elsewhere along the San Pedro margin.

Seismic-reflection line 85 (Fig. 13; location shown on Fig. 2) provides a nearly perpendicular section through the anticline and syncline. Both structures are crosscut by a swarm of normal faults that have offsets of less than about 100 m. These faults extend to within a short distance of the seafloor but do not appear to offset it. The strike of individual faults cannot be determined because of the coarse grid of seismic-reflection lines. This normal-fault zone has a peculiar orientation with respect to neighboring structures, in that it crosscuts the axes of the large anticline and syncline. Also, this zone is not obviously related to whatever rocks cause the western-shelf magnetic anomaly (magnetic data in Fig. 3, top; causative body outlined in Fig. 11). Olson (1974) described potentially analogous structures: the Wilmington anticline is cut transverse to strike by numerous small normal faults.

South of the San Pedro shelf, an important category of fault lies west of and subparallel to the Palos Verdes fault zone. For example, the northeastward view of multibeam bathymetric data (Fig. 8) shows a seafloor ridge, labeled "A," on the slope west of the Palos Verdes fault zone. Seismic-reflection sections 84 and 66 (Plate 1) show that this ridge is underlain by an anticline and by a west-dipping fault and that the anticline decreases in amplitude and radius of folding northwestward. Bathymetric data (Fig. 8) show that seafloor ridge A, and presumably its underlying fold and fault, is convex to the east. This convexity is located directly west of where normal-separation faults make up the Palos Verdes fault zone (Fig. 11). An important point is that the seafloor ridge has clearest expression and the underlying anticline has maximum relief directly west of where the Palos Verdes fault zone comprises a series of faults with normal separation. This structural arrangement, best depicted in seismic section 66 (Plate 1), suggests that these faults and folds are connected within a displacement-transfer zone, but our data are insufficient to unravel this connection.

Bathymetric data (Fig. 8) indicate that the seafloor over ridge A is unfaulted. Seismic reflection data show that locally, the trace of the fault associated with this ridge is buried by undisturbed sediment (Plate 1, section 66), but elsewhere this fault extends upward almost to the seafloor (Plate 1, section 67).

The discontinuous seafloor ridge B, revealed by bathymetric data (Fig. 8), is subparallel to and west of ridge A, and ridge B is also underlain by an anticline and west-dipping fault. Seismic section 84 (Plate 1) shows that rocks under ridge B are mainly deformed by an anticline. Section 65 (Fig. 14, section location shown on Fig. 2), however, crosses the ridge farther northwest, where faulting is more readily evident. A fault (below SP 5100 on Fig. 14) is clearly

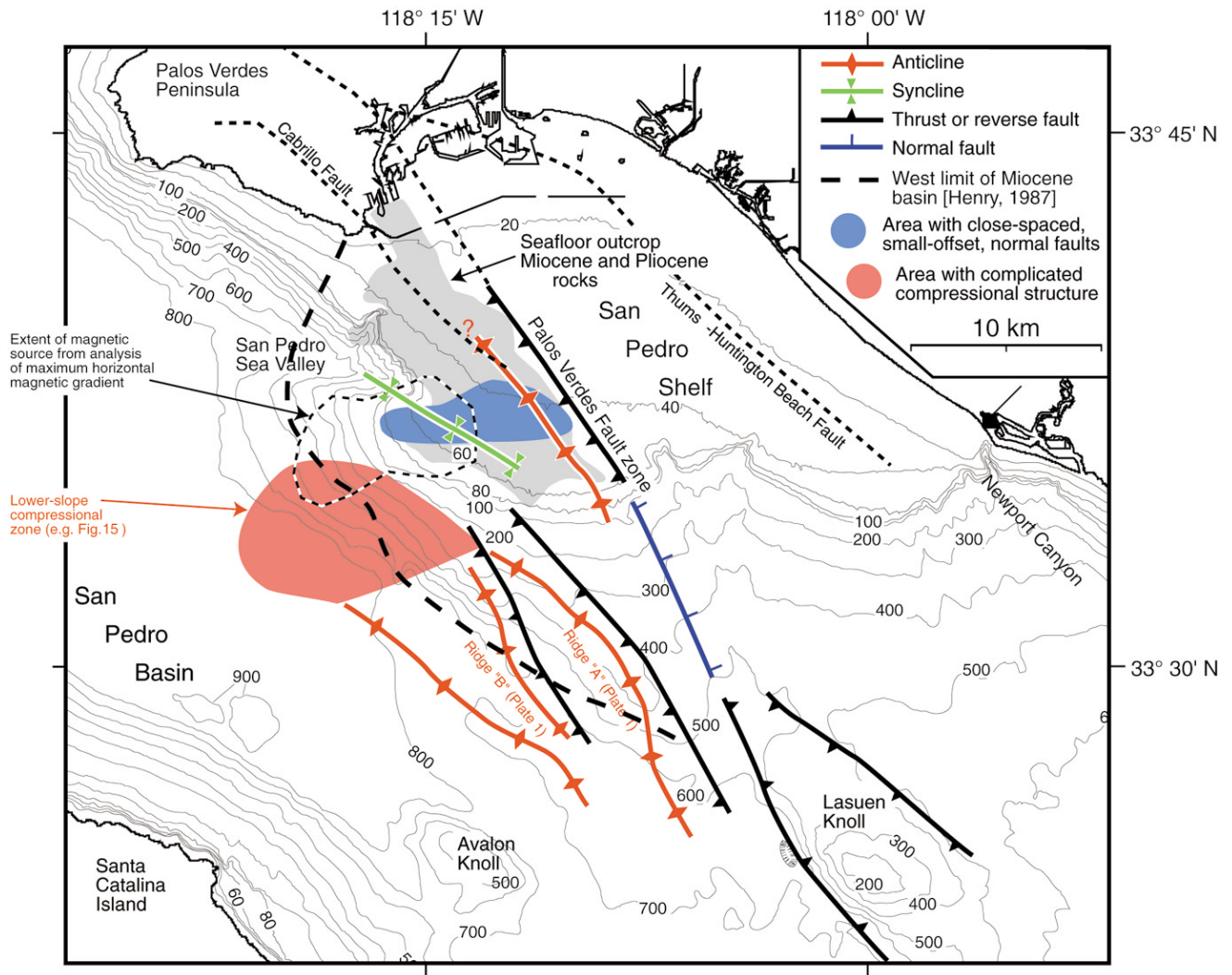


Figure 12. Summary of the main structures in the region of the San Pedro shelf and Lasuen Knoll.

expressed by the different appearance of reflections from the rock masses the fault separates. This seismic section shows that the fault dips steeply west, and this fault's tip is covered by a thin sediment drape, indicating relatively recent activity.

Rocks under the slope and west of ridge B dip west and are truncated at the seafloor along the narrow crest of the ridge (Fig. 14; seismic section 65). These rocks have the Miocene reflective appearance that was described earlier, in which the reflections are strong, parallel, uniform in appearance, and continuous over long distances. Multibeam bathymetric data (Fig. 8) show approximately where these rocks are truncated along the lower slope of the San Pedro margin. We propose that the seafloor truncation of indurated, Miocene(?) rocks evident on seismic section 65 and on other nearby sections occurred subaerially.

Rocks under the slope, between the shelf break and the flat seafloor over the San Pedro basin, produce reflections

that are continuous for about 2 km (Fig. 14, at travel times between 1.0 and 1.5 sec below SP 5700 in seismic section 65), but these rocks end abruptly to the east against a rock mass that returns only few reflections. One interpretation of this reflection geometry is that the abrupt end of reflections reveals buried relief of deep rocks, possibly metamorphic basement or Miocene volcanic rocks.

Some rocks under the slope have the Miocene reflective appearance and pinch out westward in an obvious wedge (Fig. 14, seismic sections 65 and 37). The apex of the wedge probably marks the western limit of the basin that contained the Miocene rocks. This interpretation accords with Henry (1987), who showed the regional extent of the margin of the Miocene basin near the Palos Verdes Peninsula and San Pedro shelf (basin margin is reproduced in Fig. 12). This marginal wedge and other parts of the Miocene basin have since been disrupted by oblique-slip faulting and draped over the high standing area that now makes up the San Pedro shelf.

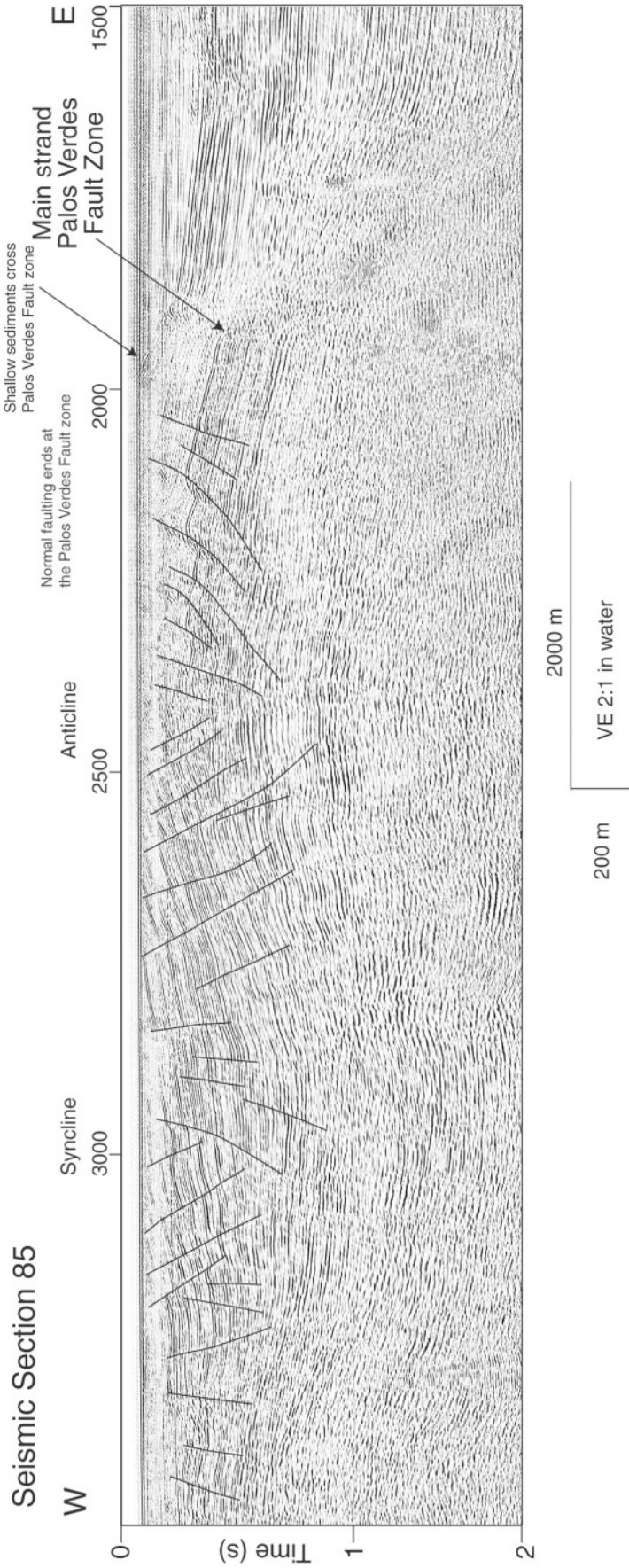


Figure 13. Detailed seismic section 85 from San Pedro shelf, showing the large anticline and syncline that border the Palos Verdes fault zone (Fig. 16). These structures are cut by numerous, small normal faults. Section location is shown in Figure 2.

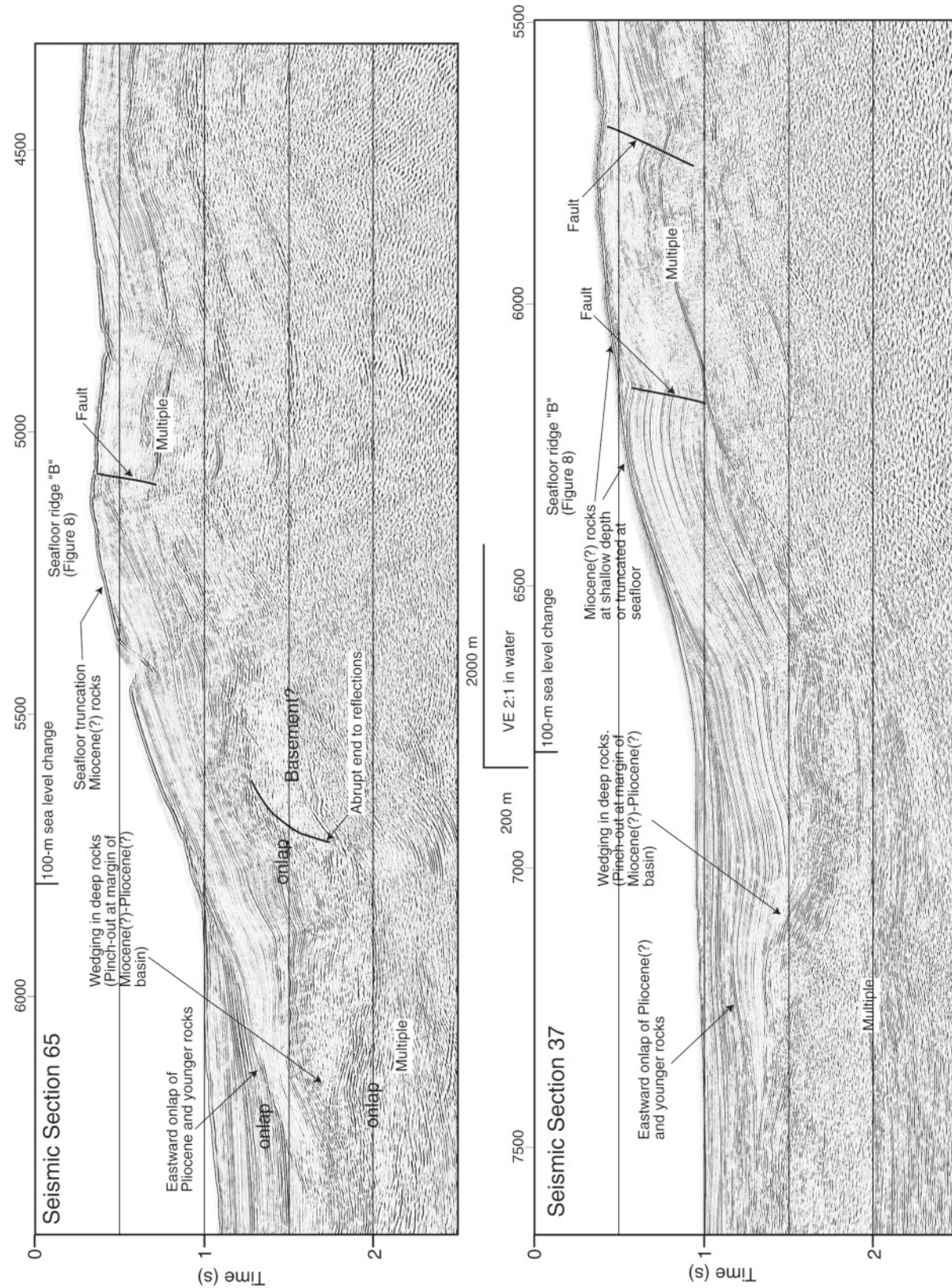


Figure 14. Seismic sections 65 and 37 over the slope west of the San Pedro shelf, showing what may be Miocene(?) rocks at shallow subsurface depth or truncated at the seafloor and the wedging of Miocene(?) rocks at the margin of the basin in which they were deposited. Location of sections is shown in Figure 7.

The lower-slope compressional zone (Fig. 12) includes complicated, compressional deformation of rocks that underlie the slope and a small part of the San Pedro basin (Fig. 15; location of seismic section 115 is shown in Fig. 2). This compressional zone is about 8 km wide, and structural growth therein has produced a complicated stratigraphy with numerous unconformities and other bed truncations. Folds and thrust faults within the zone appear to belong to two generations. Some deep-seated faults, like the one below SPs 3800 (Fig. 15), appear to be inactive because they do not extend upward to deform rocks at or at near the seafloor. Other faults (e.g., below SPs 3000 and 3500; Fig. 15) are part of a younger generation that arches the seafloor and deforms shallow sediment. Seismic-reflection data available to us lack the penetration to determine how these structures are related at depth, but we propose that they merge into a decollement.

Discussion

Potential-Field Modeling

Gravity and magnetic models of the isolated, pronounced aeromagnetic anomaly over the western San Pedro shelf (Fig. 3) reveal the presence of a large magnetic body. Assuming reasonable magnetizations, which are based on measurements made on a wide variety of rock samples, the resulting magnetic models (Fig. 16) indicate that a large mass, as thick as 5.5 km, of magnetic rock underlies the outer part of the San Pedro shelf. Susceptibility values in the model as high as 0.0019×10^{-3} cgs units indicate that these rocks are moderately to strongly magnetic. Sedimentary rocks are usually weakly magnetic and are unlikely sources for the magnetic anomaly. Catalina schist forms the crystalline basement in this region but does not produce significant aeromagnetic anomalies where it is exposed on Catalina Island. The most likely source for the anomaly is middle Miocene basalt. In support of the idea that the magnetic source is basalt, we note that a high-amplitude aeromagnetic anomaly is located just west of the Palos Verdes Peninsula (Fig. 3), and an oil well located within the aeromagnetic anomaly encountered at least a 1-km thickness of basalt (Dibblee, 1999). This implies that a significant thickness of basalt is needed to produce a large aeromagnetic anomaly like the one measured over the outer San Pedro shelf.

The gravity map and models indicate that the magnetic source rocks do not produce an associated gravity high. However, density measurements on samples of Tertiary basalt near the Los Angeles basin indicate a low average density of only 2.58 g/cm^3 (29 samples), which is substantially less dense than the Catalina schist. In our opinion, the lack of an gravity high associated with the outer-shelf magnetic anomaly results from the basalt's low density.

The inferred mass of basalt may have affected the style of deformation of sedimentary rocks that encase the basalt. The mass of magnetic rocks; the lower-slope compressional

zone, which extends along the southwest margin of the magnetic rocks; and the puzzling east–west zone of numerous, small, normal faults, which lie along the east margin of the basalt(?) (Figs. 13 and 14), may be linked genetically. For example the distribution of compressive and extensional faulting (Fig. 11) could have resulted from clockwise rotation and perhaps westward translation of the basalt(?) relative to its encasing sedimentary rock.

Faults and Earthquake Hazards

To fully understand the earthquake threat posed by offshore faults near Los Angeles requires that substantial interpretive differences be resolved that now persist among researchers. For example, Namson and Davis (1990) and Shaw and Suppe (1996), among others, assumed that only limited strike-slip movement occurs along major faults; they postulated instead that mainly thrust or reverse movement occurs at depth along blind faults. Such faults are commonly expressed at Earth's surface as broad folds and as discontinuous fault strands that may have styles of deformation and offset that are dissimilar to what occurs along the deeper, master faults. Hypocenters 8–12 km deep are interpreted to lie along a down-dip, southwestward projection of the Palos Verdes fault zone (Shaw [1999]; shown in Fig. 6, bottom); the aligned hypocenters show mainly reverse fault movement in this depth range. Other researchers, however, emphasized the importance of strike- or oblique-slip offset (e.g., Nardin and Henyey, 1978; Wright, 1991; Francis *et al.*, 1996; McNeilan *et al.*, 1996; Bohannon and Geist, 1998). According to this view, movement along the Palos Verdes fault zone is mainly strike slip and large positive structures have developed along it, possibly owing to restraining bends in the fault zone.

The controversy about predominant slip mode along faults remains unresolved because data presented here do not reveal sufficiently deep structural levels to unravel the relationships among offshore faults. In our view, however, the diversity in the near-surface structural expression of the Palos Verdes fault zone is best explained by movement along a deep strike-slip fault.

Using seismic-reflection data presented herein, we divide the offshore stretch of the Palos Verdes fault zone into three segments that are based on the fault zone's structure in the upper 2 km of the crust. The northwestern segment underlies the San Pedro shelf (Fig. 16), where the shallow fault zone is vertical or dips steeply west. The middle fault-zone segment underlies the bathymetric saddle that separates the San Pedro shelf from Lasuen Knoll. The fault zone in this segment is made up of east-dipping faults with normal separation. Near Lasuen Knoll the southeastern segment of the Palos Verdes fault zone shows reverse separation and locally dips east at shallow angles, but along much of the knoll's west scarp the fault zone appears to dip steeply.

The northwest segment of the Palos Verdes fault zone evidently deforms young rocks and the seafloor (McNeilan *et al.*, 1996; Clarke *et al.*, 1998). Some high-resolution seis-

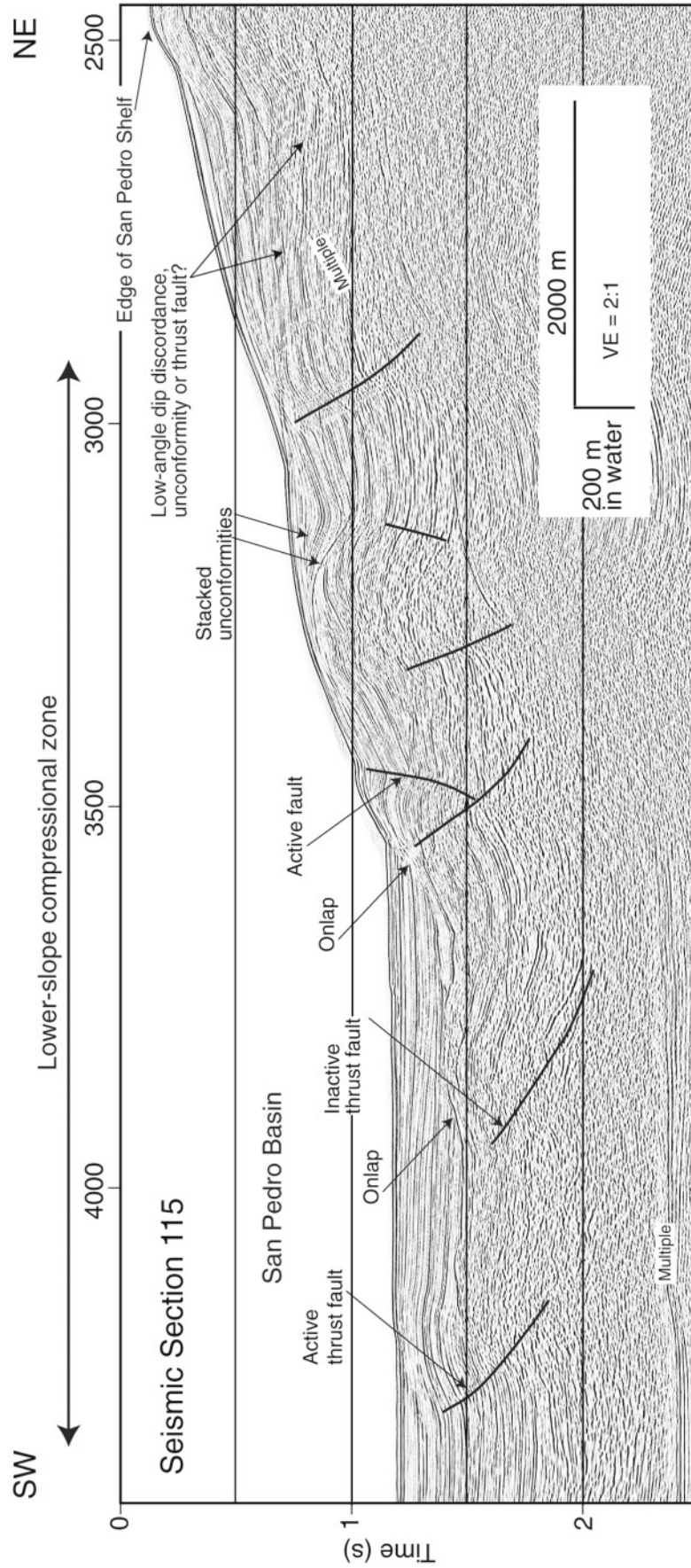


Figure 15. Seismic section 115 over the slope west of the San Pedro shelf, showing the lower-slope compressional zone. Section location is shown in Figure 2.

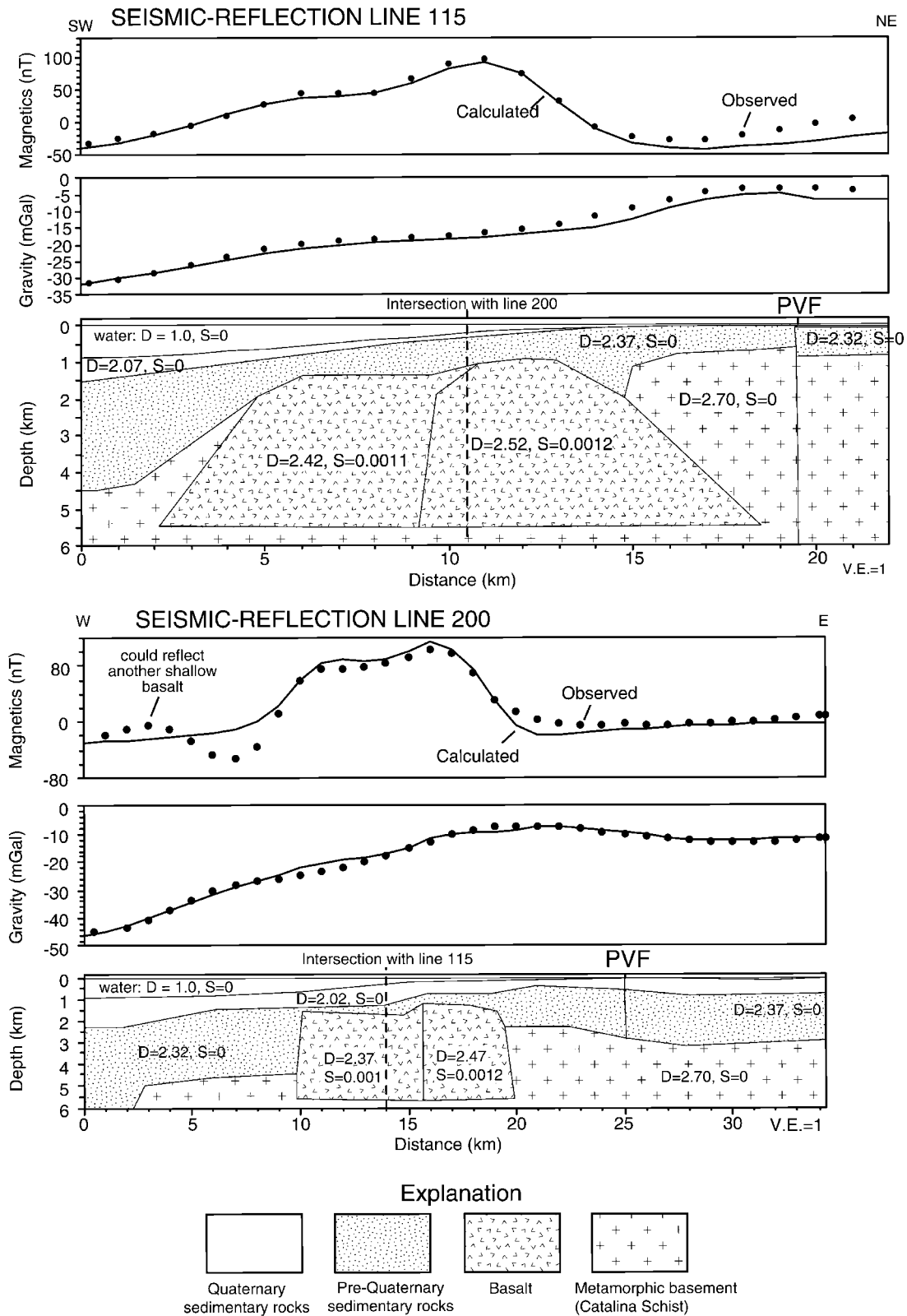


Figure 16. 2.5-dimensional magnetic and gravity models along seismic sections 200 (top) and 115 (bottom). "D" refers to the density of the body in grams per cubic centimeter; "S" is the susceptibility assigned to the body in 10^{-3} cgs units. PVF, Palos Verdes fault zone. Differences in physical properties assigned to the magnetic body can be attributed to inadequate modeling of the three-dimensionality of the source.

mic-reflection data (Francis *et al.*, 1996) reveal a restraining bend and attendant flower structure along this part of the fault zone that coincides with a low seafloor swale about 1–4 m high. This deformation apparently postdates submergence and erosion of the shelf during the past 10 ka. Seismic-reflection data presented here indicate that shallow fill in the Wilmington graben is offset by the fault zone. This fill extends across this zone and overlies truncated Miocene rocks southwest of the fault zone.

The middle segment of the Palos Verdes fault zone includes normal-separation faults under the part of the continental slope that deepens southeastward from the San Pedro shelf. These fault segments extend downward at least 1–2 km into the crust. These normal faults may have developed analogously to faults in the Inglewood oil field, which is located along the strike-slip Newport–Inglewood fault (figures 19 and 20 of Wright [1991]). There, a central graben developed in the upper 1 km of the crust, at the crest of an anticline, where the main and underlying, strike-slip fault undergoes a minor (about 2°–5°) change in strike. We propose that the normal-separation faults in the middle segment of the Palos Verdes fault zone probably formed within a releasing bend along a right-lateral strike-slip fault.

The middle segment of the Palos Verdes fault zone ends abruptly between San Pedro shelf and Lasuen Knoll, and near this end, the modern San Gabriel Canyon is incised into the upper plate of the Palos Verdes fault zone, close to the fault zone's trace (Fig. 9). Seismic-reflection data indicate that the channel has been in this position while the upper part of the sediment along the fault's east side was being deposited over a prominent unconformity. These observations require that as the channel meandered laterally, movement along the Palos Verdes fault zone involved little or no vertical separation; otherwise the channel would have been diverted elsewhere. This limitation does not preclude pure strike-slip movement along the fault zone, but the reverse fault under the channel (Fig. 9) has had little or no vertical movement.

Along the southeast segment of the Palos Verdes fault zone, sharp seafloor scarps that border Lasuen Knoll, possible tilted wave-cut terraces, and disrupted shallow sediment all attest to recent fault movement. Lasuen Knoll appears to be underlain by a pop-up structure, like those that develop along a restraining bend or step-over in a strike-slip fault system.

Probable wave-cut terraces and fresh fault scarps evident near Lasuen Knoll indicate a complex history of vertical motion that will hinder efforts to decipher recent fault offset. The shallow unconformity along the west side of the Palos Verdes fault zone at Lasuen Knoll (Fig. 9) suggests a sequence of events that includes sediment deposition, uplift, erosion, and then subsidence. The sharp fault scarps bordering Lasuen Knoll indicate relatively recent uplift that postdates the final subsidence.

The Cabrillo fault (Fig. 12) extends at least as far offshore, southeast from the Palos Verdes Peninsula, as seis-

mic-reflection line 115, as indicated by Marlow *et al.* (2000). In our seismic-reflection data, this fault lies along an obvious and abrupt change in the appearance of reflections from Miocene rocks, but the fault cannot be followed with certainty southeast of line 115.

A maze of reverse faults that forms the lower-slope compressional zone (Fig. 15) appears to be restricted to the area of the margin that lies west of the San Pedro shelf. Whether or not these discontinuous faults connect with deeper, more extensive faults that would constitute an earthquake hazard cannot be determined using our data.

Offshore faults that parallel the Palos Verdes fault zone include those that developed along with seafloor ridges A and B (Plate 1). Ridge A has its greatest structural development due west of where normal-separation faults make up the Palos Verdes fault zone. These faults are probably linked in the subsurface and must be considered as a whole when evaluating earthquake hazards.

Conclusion

1. Geological and geophysical data reveal the structural geology and earthquake hazards of the area just offshore from the Los Angeles urban region. Prominent structures include the Wilmington graben, the Palos Verdes fault zone, and faults below the west part of the shelf and slope.
2. In the shallow (>2 km) crust, the Palos Verdes fault zone includes three segments. Under the San Pedro shelf, the main fault strand in this zone dips west and is probably an oblique-slip fault. Southeast of the shelf, the fault zone comprises several normal-separation faults, most of which dip east. Near Lasuen Knoll, the Palos Verdes fault zone exhibits reverse separation and dips east at a low angle, and what appear to be fresh seafloor scarps indicate recent fault movement. This segmentation probably results from changes in geometry along a master, right-lateral, strike-slip fault zone at depth. This segmentation could complicate efforts to apportion seismic hazard along this fault zone because changes in fault geometry could effect dynamic earthquake rupture.
3. Rocks under Lasuen Knoll and those under the Palos Verdes Peninsula are involved in oblique deformation and uplift. The relief of Lasuen Knoll and some secondary faults associated with this knoll terminate abruptly northward along a bathymetric scarp that is transverse to the Palos Verdes fault zone. In like fashion, the high relief of the Palos Verdes Peninsula ends abruptly along the south shore of Santa Monica Bay. Perhaps structures under the peninsula end along a transverse fault like the transverse one near Lasuen Knoll.
4. Seismic-reflection and multibeam bathymetric data reveal the extent of several northwest-striking faults under the outer shelf and slope. These faults deform rocks into anticlines that have clear geomorphic expression as seafloor ridges. Evidence for recent movement along these

faults is equivocal, however, because at many locations undated sediment just under the seafloor appears to be undeformed.

5. Significant tsunamis can result from major submarine landslides, and the debris from one or more landslides is evident along the axis of the San Pedro Sea Valley. This sea valley follows the axis of a large syncline under the San Pedro shelf, so that synclinal rocks, of probable Miocene and Pliocene age, dip toward the axis of the sea valley. This indicates that more landslides, and hence tsunamis, could occur because the synclinal rocks dip favorably for the development of coherent slide masses.
6. The stratigraphy under the San Pedro shelf, derived using seismic-reflection data as well as information from oil wells and seafloor samples, indicates that east of the Palos Verdes fault zone, the Wilmington graben contains thick (as much as 1.5 km) Quaternary deposits, whereas west of the fault zone, Miocene and Pliocene rocks are truncated at the seafloor. Rocks under the slope are assigned provisional, Miocene and Pliocene ages on the basis of the appearance of seismic reflections. These provisionally dated rocks under the slope end in the west in a wedge that probably marks the margin of the basin in which these rocks were deposited.
7. Modeling of aeromagnetic data reveals a large magnetic body under the west part of the San Pedro shelf and the adjacent upper slope. This body is probably Miocene basalt. The basalt may be more competent than its encasing sedimentary rocks, which could explain the distribution of local structures arrayed around the magnetic mass.

Acknowledgments

We thank Gary Fuis, Daniel Ponti, and Thomas Brocher for critical comments on this article. Craig Nicholson was especially helpful in focusing the presentation of results in this article. Christina Gutmacher, Florence Wong, and Carolyn Degnan assisted our effort greatly in data collection, processing, and display.

References

- Astiz, L., and P. M. Shearer (2000). Earthquake locations in the inner Continental Borderland, offshore southern California, *Bull. Seism. Soc. Am.* **90**, 425–449.
- Atwater, T., and J. Stock (1998). Neogene plate tectonic history of southwestern United States: an update, in *New Zealand Geophysical Society 1998 Joint Annual Conference: Programme and Abstracts*, Geol. Soc. New Zealand Misc. Pub. 101A, 31.
- Barron, J. A., and C. M. Isaacs (2001). Updated chronostratigraphic framework for the California Miocene, in *The Monterey Formation from Rocks to Molecules*, Isaacs C. M. and J. Rullkötter (Editors), Columbia U Press, New York, 393–395.
- Barrows, A. G. (1974). A review of the geology and earthquake history of the Newport–Inglewood structural zone, southern California, Calif. Div. Mines and Geol. Sp. Rept. 114, 115 pp.
- Bohannon, R. G., and E. L. Geist (1998). Upper crustal structure and Neogene tectonic development of the California Continental Borderland, *Geol. Soc. Amer. Bull.* **110**, 779–800.
- Brocher, T. M., R. W. Clayton, K. D. Klitgord, R. G. Bohannon, R. Sliter, J. K. McRaney, J. V. Gardner, and J. B. Keene (1995). *Multichannel Seismic-Reflection Profiling on the R/V Maruice Ewing during the Los Angeles Region Seismic Experiment (LARSE), California, U.S. Geol. Surv. Open-File Rept. 95-228*, 70 pp.
- Bryan, M. E. (1987). Emergent marine terraces and Quaternary tectonics, Palos Verdes Peninsula, California, in *Geology of the Palos Verdes Peninsula and San Pedro Bay*, P. J. Fischer (Editor), Pacific Section SEPM and AAPG Field Trip Guide Book 55, SEPM, Tulsa, Oklahoma, 63–78.
- Clarke, S. H., and M. P. Kennedy (1998). Analysis of late Quaternary faulting in the Los Angeles Harbor area and hazard to the Vincent Thomas Bridge, California Dept. of Conservation, Division of Mines and Geology Open-File Rept. 98-01, 50 pp.
- Conrad, C. L., and P. L. Ehlig (1987). The Monterey Formation of the Palos Verdes Peninsula, California: an example of sedimentation in a tectonically active basin within the California Continental Borderland, in *Geology of the Palos Verdes Peninsula and San Pedro Bay*, P. J. Fischer (Editor), Pacific Section SEPM and AAPG Field Trip Guide Book 55, SEPM, Tulsa, Oklahoma, 17–30.
- Crouch, J. K., and J. Suppe (1993). Late Cenozoic tectonic evolution of the Los Angeles basin and inner California borderland: a model for core complex-like crustal extension, *Geol. Soc. Am. Bull.* **105**, 1415–1434.
- Davis, T., and J. Namson (2002). Nine regional cross-sections across the Los Angeles Basin, www.davisnamson.com/downloads/index.htm (last accessed March 2004).
- Dibblee, T. W., Jr. (1999). Geologic map of the Palos Verdes Peninsula and vicinity, Redondo Beach, Torrance, and San Pedro quadrangles, Los Angeles County, California: Dibblee Geological Foundation map DF-70, scale 1:24,000.
- Dickinson, W. R. (1997). Tectonic implications of Cenozoic volcanism in coastal California, *Geol. Soc. Am. Bull.* **109**, 936–954.
- Dolan, J. F., K. Sieh, and T. K. Rockwell (2000). Late Quaternary activity and seismic potential of the Santa Monica fault system, Los Angeles, California, *Geol. Soc. Am. Bull.* **112**, 1559–1581.
- Fischer, P. J. (1992). Neotectonics of the Newport–Inglewood and Palos Verdes fault zones along the offshore margins of the greater Los Angeles basin, in *Proc. of the 35th Annual Meeting*, M. L. Stout (Editor), Assoc. Engineering Geol. Long Beach, California 1012-9/1992, 603–615.
- Fischer, P. J., R. H. Patterson, C. Darrow, J. H. Rudat, and G. Simila (1987). The Palos Verdes fault zone: onshore to offshore, in *Geology of the Palos Verdes Peninsula and San Pedro Bay*, P. J. Fischer (Editor), Pacific Section SEPM and AAPG Field Trip Guide Book 55, SEPM, Tulsa, Oklahoma, 91–133.
- Fisher, M. A., W. R. Normark, R. G. Bohannon, R. Sliter, and A. J. Calvert (2003). Geology of the continental margin beneath Santa Monica Bay, southern California, from seismic-reflection data, *Bull. Seism. Soc. Am.* **93**, 1955–1983.
- Francis, R. D., M. R. Legg, D. R. Sigurdson, and P. J. Fischer (1996). Restraining bend along the Palos Verdes fault zone, offshore southern California, *EOS* **77**, no. 46, 512.
- Gardner, J. V., and P. Dartnell (2002). *Multibeam Mapping of the Los Angeles, California Margin*, U.S. Geol. Surv. Open-File Rept. OF02-162.
- Greene, H. G., and M. P. Kennedy (Editors) (1987). Geology of the inner southern California continental margin, California Division of Mines and Geology, California Continental margin Geologic Map Series, scale 1:250,000.
- Gutmacher, C. E., W. R. Normark, S. L. Ross, B. D. Edwards, R. Sliter, P. Hart, B. Cooper, J. Childs, and J. A. Reid (2000). *Cruise Report for AI-00-SC Southern California Earthquake Hazards Project*, Part A, U.S. Geol. Surv. Open-File Rept. 00-516, 67 pp.; <http://geopubs.wr.usgs.gov/open-file/of00-516/of00-516p.pdf> (last accessed March 2004).
- Hauksson, E., and S. J. Gross (1991). Source parameters of the 1933 Long Beach earthquake, *Bull. Seism. Soc. Am.* **81**, 81–98.
- Hauksson, E., and G. V. Saldivar (1986). The 1930 Santa Monica and the

- 1979 Malibu, California, earthquakes, *Bull. Seism. Soc. Am.* **76**, 1542–1559.
- Henry, M. J. (1987). Los Angeles basin: an overview, in *Geologic Field Guide to the Long Beach Area*, D. Clarke and C. Henderson (Editors), Pacific Section AAPG Field Trip Guide Book 58, 1–29.
- Johnson, D. A., and A. V. Acosta (1989). *Strong-Motion Data from the Malibu, California, Earthquake of January 19, 1989*, U.S. Geol. Surv. Open-File Rept. OF 89-0186, 21 pp.
- Kamerling, M. J., and B. P. Luyendyk (1985). Paleomagnetism and Neogene tectonics of the northern Channel Islands, California, *J. Geophys. Res.* **90**, 12,485–12,502.
- Langenheim, V. E., P. F. Halvorson, E. L. Castellanos, and R. C. Jachens (1993). *Aeromagnetic Map of the Southern California Borderland East of the Patton Escarpment*, U.S. Geol. Surv. Open-File Rept. 93-250, scale 1:500,000.
- Legg, M. R., O. V. Wong, and F. Suarez-Vidal (1991). Geologic structure and tectonics of the inner continental borderland of northern Baja California, in *The Gulf and Peninsular Province of the Californias*, J. P. Dauphin and R. T. Bernd (Editors), American Association of Petroleum Geologists Memoir 47, 145–177.
- Locat, J., and H. J. Lee (2002). Submarine landslides: advances and challenges, *Can. Geotech. J.* **39**, 193–212.
- Luyendyk, B. P., M. J. Kamerling, and R. R. Terres (1980). Geometric model for Neogene crustal rotations in southern California, *Geol. Soc. Am. Bull.* **91**, 211–217.
- Marlow, M. S., J. V. Gardner, and W. R. Normark (2000). Using high-resolution multibeam bathymetry to identify seafloor surface rupture along the Palos Verdes fault zone complex in offshore southern California, *Geology* **28**, 587–590.
- McNeilan, T. W., T. K. Rockwell, and G. Resnik (1996). Style and rate of Holocene slip, Palos Verdes fault zone, southern California, *J. Geophys. Res.* **101**, 8317–8334.
- Namson, J. S., and T. L. Davis (1990). Late Cenozoic fold and thrust belt of the southern Coast Ranges and Santa Maria basin, California, *Am. Assoc. Petrol. Geol. Bull.* **74**, 467–492.
- Nardin, T. R., and T. L. Henyey (1978). Pliocene–Pleistocene diastrophism of Santa Monica and San Pedro shelves, California continental borderland, *Am. Assoc. Petrol. Geol. Bull.* **62**, 247–272.
- Nicholson, C., C. Sorlien, T. Atwater, J. C. Crowell, and B. P. Luyendyk (1994). Microplate capture, rotation of the western Transverse Ranges, and initiation of the San Andreas transform as a low-angle fault system, *Geology* **22**, 491–495.
- Normark, W. R., R. G. Bohannon, R. Sliter, G. Dunhill, D. W. Scholl, J. Laursen, J. A. Reid, and D. Holton (1999a). *Cruise Report for A1-98-SC Southern California Earthquake Hazards Project*, U.S. Geol. Surv. Open-File Rept. 99-152, 60 pp.
- Normark, W. R., J. A. Reid, R. W. Sliter, D. Holton, C. E. Gutmacher, M. A. Fisher, and J. R. Childs (1999b). *Cruise Report for 01-99-SC: Southern California Earthquake Hazards Project*, U.S. Geol. Surv. Open-File Rept. 99-560, <http://geopubs.wr.usgs.gov/open-file/of99-560/> (last accessed March 2004).
- Normark, W. R., R. Sliter, and M. McGann (2002). Emplacement of the 7,500 yr B.P. Palos Verdes submarine debris avalanche, southern California, *EOS* (Fall Meeting Supp.) **83**, no. 47, T71E-1219.
- Olson, L. J. (1974). Belmont oil field, California Department of Conservation, Division of Oil and Gas Publication TP01, Sacramento, California, 1–14.
- Rivero, C., J. H. Shaw, and K. L. Mueller (2000). Oceanside and Thirtymile Bank blind thrusts: implications for earthquake hazards in coastal southern California, *Geology* **28**, 891–894.
- Shaw, J. H. (1999). Annual Report, 1999, to the Southern California Earthquake Center: Seismic-reflection transect and geologic cross-section across the central Los Angeles basin and San Pedro Bay; www.scec.org/research/99research/99shaw.pdf (last accessed March 2004).
- Shaw, J. H., and J. Suppe (1996). Earthquake hazards of active blind-thrust faults under the central Los Angeles basin, California, *J. Geophys. Res.* **101**, 8623–8642.
- Stanley, R. G., D. S. Wilson, and P. A. McCrory (2000). *Locations and Ages of Middle Tertiary Volcanic Centers in Coastal California*, U.S. Geol. Surv. Open-File Rept. 00-154, 27 pp.
- ten Brink, U. S., J. Zhang, T. M. Brocher, D. A. Okaya, K. D. Klitgord, and G. S. Fuis (2000). Geophysical evidence for the evolution of the California inner continental borderland as a metamorphic core complex, *J. Geophys. Res.* **105**, 5835–5857.
- Truex, J. N. (1973). Structural evolution of Wilmington anticline, California (abstract), *Am. Assoc. Petrol. Geol. Bull.* **57**, 809.
- Ward, S. N., and G. Valensise (1994). The Palos Verdes terraces, California: bathtub rings from a buried reverse fault, *J. Geophys. Res.* **99**, 4485–4494.
- Woodring, W. P., M. N. Bramlette, and W. S. W. Kew (1946). Geology and paleontology of the Palos Verdes Hills, California, *U.S. Geol. Surv. Profess. Pap.* 207, 145 pp.
- Wright, T. L. (1991). Structural geology and tectonic evolution of the Los Angeles Basin, California, in *Active Margin Basins*, K. T. Biddle (Editor), American Association Petroleum Geologists Memoir 52, 35–134.
- U.S. Geological Survey
Coastal and Marine Geology Team
345 Middlefield Road, MS 999
Menlo Park, California 94025
mfisher@usgs.gov
(M.A.F., W.R.N., R.S.)
- U.S. Geological Survey
Earth Surface Processes Team
345 Middlefield Road
Menlo Park, California 94025
(V.E.L.)
- Department of Earth Sciences
Simon Fraser University
Burnaby, B.C. V5A 1S6, Canada
(A.J.C.)